www.coinweb.no

SINTEF Building and Infrastructure Gro Markeset and Roar Myrdal

Modelling of reinforcement corrosion in concrete - State of the art

COIN Project report 7 - 2008

SINTEF

SINTEF Building and Infrastructure

Gro Markeset and Roar Myrdal

Modelling of reinforcement corrosion in concrete - State of the art

COIN P4 Operational service life design

SP 4.1 F Service life modelling and prediction

COIN Project report 7 – 2008

COIN Project report no 7
Gro Markeset and Roar Myrdal
Modelling of reinforcement corrosion in concrete - State of the art
COIN P4 Operational service life design
SP 4.1 F Service life modelling and prediction

Keywords:
Materials technology, Concrete, Corrosion, Reinforcement, Modelling

ISSN 1891-1978 (online)
ISBN 978-82-536-1073-3 (printed)
ISBN 978-82-536-1081-8 (pdf)

20 copies printed by AIT AS e-dit

Content: 100 g Scandia
Cover: 240 g Trucard

Address: Forskningsveien 3 B
POBox 124 Blindern
N-0314 OSLO
Tel: +47 22 96 55 55
Fax: +47 22 69 94 38 and 22 96 55 08

www.sintef.no/byggforsk
www.coinweb.no

Cooperation partners / Consortium Concrete Innovation Centre (COIN)

Aker Solutions
Contact: Jan-Diederik Advocaat
Email: jan-diederik.advocaat@akersolutions.com
Tel: +47 67595050

Borregaard Ligno Tech
Contact: Kåre Reknes
Email: kare.reknes@borregaard.com
Tel: +47 69118000

maxit Group AB
Contact: Geir Norden
Email: geir.norden@maxit.no
Tel: +47 22887700

Norcem AS
Contact: Terje Rønning
Email: terje.ronning@norcem.no
Tel: +47 35572000

NTNU
Contact: Terje Kanstad
Email: terje.kanstad@ntnu.no
Tel: +47 73594700

Rescon Mapei AS
Contact: Trond Hagerud
Email: trond.hagerud@resconmapei.no
Tel: +47 69972000

SINTEF Building and Infrastructure
Contact: Tor Arne Hammer
Email: tor.hammer@sintef.no
Tel: +47 73596856

Skanska Norge AS
Contact: Sverre Smeplass
Email: sverre.smeplass@skanska.no
Tel: +47 40013660

Spenncon AS
Contact: Ingrid Dahl Hovland
Email: ingrid.dahl.hovland@spenncon.no
Tel: +47 67573900

Norwegian Public Roads Administration
Contact: Kjersti K. Dunham
Email: kjersti.kvalheim.dunham@vegvesen.no
Tel: +47 22073940

Unicon AS
Contact: Stein Tosterud
Email: stto@unicon.no
Tel: +47 22309035

Veidekke Entreprenør ASA
Contact: Christine Hauck
Email: christine.hauck@veidekke.no
Tel: +47 21055000

Summary

A literature review has been made with respect to the basics of steel reinforcement corrosion and the subsequent formation of cracks in the concrete cover generated by the expansion of corrosion products. Models describing the corrosion and concrete deterioration processes are covered.

Several formulae and models have been proposed for the calculation of the time to onset of cracking of the concrete cover caused by the reinforcement corrosion. Some analytical models are deduced from electrochemical and mechanical principles and some empirical expressions are obtained according to experimental data fitting.

Various studies show considerable variations in the extent of corrosion required to initiate cracking and the influence of cover thickness and steel bar diameter. So far the models for crack initiation and propagation have been restricted to the stresses generated by the expansion of corrosion products. Models comprising the total complexity of the problem, especially generated by load induced stresses, have not been found.

Further research should focus on developing models based on electrochemical, chemical, physical and mechanical parameters only, without introducing numerical coefficients to fit empirical data.

Oslo, 2008

Tor Arne Hammer
Centre Manager

Gro Markeset, Roar Myrdal

Foreword

COIN - Concrete Innovation Centre - is one of presently 14 Centres for Research based Innovation (CRI), which is an initiative by the Research Council of Norway. The main objective for the CRIs is to enhance the capability of the business sector to innovate by focusing on long-term research based on forging close alliances between research-intensive enterprises and prominent research groups.

The vision of COIN is creation of more attractive concrete buildings and constructions. Attractiveness implies aesthetics, functionality, sustainability, energy efficiency, indoor climate, industrialized construction, improved work environment, and cost efficiency during the whole service life. The primary goal is to fulfill this vision by bringing the development a major leap forward by more fundamental understanding of the mechanisms in order to develop advanced materials, efficient construction techniques and new design concepts combined with more environmentally friendly material production.

The corporate partners are leading multinational companies in the cement and building industry and the aim of COIN is to increase their value creation and strengthen their research activities in Norway. Our over-all ambition is to establish COIN as the display window for concrete innovation in Europe.

About 25 researchers from SINTEF (host), the Norwegian University of Science and Technology - NTNU (research partner) and industry partners, 15 - 20 PhD-students, 5 - 10 MSc-students every year and a number of international guest researchers, work on presently 5 projects:

- Advanced cementing materials and admixtures
- Improved construction techniques
- Innovative construction concepts
- Operational service life design
- Energy efficiency and comfort of concrete structures

COIN has presently a budget of NOK 200 mill over 8 years (from 2007), and is financed by the Research Council of Norway (approx. 40 %), industrial partners (approx 45 %) and by SINTEF Building and Infrastructure and NTNU (in all approx 15 %). The present industrial partners are:

Aker Kværner Engineering and Technology, Borregaard LignoTech, maxitGroup, Norcem A.S, Norwegian Public Roads Administration, Rescon Mapei AS, Spenncon AS, Unicon AS and Veidekke ASA.

For more information, see www.coinweb.no

TABLE OF CONTENTS

1 Introduction

Reinforcement corrosion has been identified as being the predominant deterioration mechanism for reinforced concrete structures, which seriously affects the serviceability and the safety of the structures.

Deterioration caused by reinforcement corrosion is normally divided into two main time periods, the initiation period and the propagation period, se Fig. 1.1. The initiation period is defined as the time until the reinforcement becomes depassivated either by the presence of chloride salts or by carbonation. As soon as the concrete at the depth of the reinforcement is carbonated or contains a critical amount of free chlorides the reinforcement becomes depassivated and corrosion may occur. This limit state defines the beginning of the propagation period. During the propagation period the reinforcement is corroding, which may lead to deterioration of the concrete as well. Expansive corrosion products provoke cracks along the reinforcement, and subsequently, spalling of the concrete cover may occur. Finally, the loss of cross section of the reinforcement may lead to reduction of the load bearing capacity.

This state-of-the-art report gives an overview of models describing the corrosion process in reinforced concrete and the subsequent formation of cracks of the concrete cover generated by the expansion of corrosion products. A quantitative prediction of the time to cracking is important in the development of an overall deterioration model for the prediction of service life.

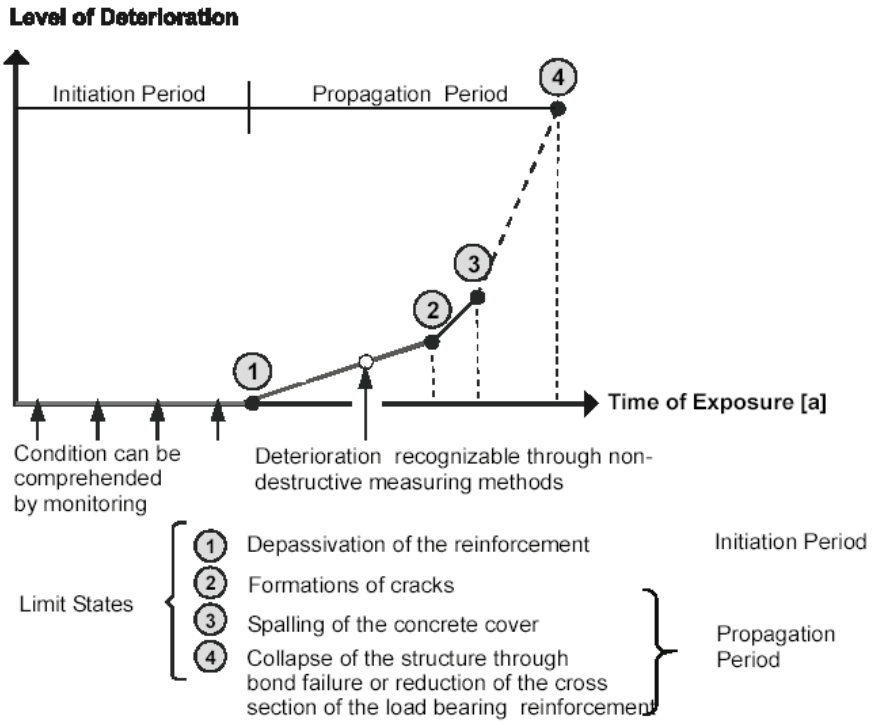

Figure 1.1 Typical deterioration levels for a steel reinforced concrete structure suffering from corrosion [***fib*** 2006].

2 Basics of corrosion

2.1 Reaction mechanisms and kinetics

Iron and plain carbon steels (iron alloyed with small amounts of carbon) are thermodynamically unstable materials. Nature will bring these materials back to their original and thermodynamically stable forms, namely oxides, i.e. rust-like materials. Under neutral and basic conditions, as in concrete, the process from steel to oxides/rust requires the presence of both water and oxygen. Water and oxygen act as chemical 'driving forces'. This process is provided by electrochemical reactions, i.e. chemical reactions involving transfer of electrons and electric charges at the interface between the metal and the water. Different types of iron oxides may be formed depending on exposure conditions:

Steel	+	Water	+	Oxygen	→	Iron oxides/rust	
Fe		H_2O		O_2		$Fe(OH)_2$ / Fe_3O_4 / Fe_2O_3/…	(2.1)

This overall reaction may be divided into two reactions, called half-cell reactions, which are running simultaneously at adjacent locations, often very close to each other (microscopic distances), or separated by macroscopic distances. Two sites very close to each other may even alternate as scenes for the two half-cell reactions.

One of the half-cell reactions, called the anodic reaction, is the dissolution of iron, i.e. an oxidation of iron to form ferrous ions and leaving behind electrons in the metal:

Anodic reaction – oxidation of iron

$$Fe = Fe^{2+} + 2\,e^- \tag{2.2}$$

Iron is oxidised from Fe (oxidation state 0) to Fe^{2+} (oxidation state +2).

In the other half-cell reaction, called the cathodic reaction, the liberated electrons from the oxidation of iron are consumed by oxygen in the presence of water to form hydroxyl (OH^-). In this reaction oxygen is electrochemically reduced from O_2 (oxidation state 0) to OH^- (oxidation state –2):

Cathodic reaction – reduction of oxygen

$$O_2 + H_2O + 2e^- = 2\,OH^- \tag{2.3}$$

If there is no external electric source of electrons, the anodic reaction must generate electrons at exactly the same rate as the cathodic reaction consumes them.

The algebraic sum of these two reactions makes the total reaction, called the corrosion cell reaction:

$$Fe_{steel} + O_2 + H_2O = Fe^{2+}{}_{dissolved} + 2\,OH^- \tag{2.4}$$

Ferrous hydroxide ($Fe(OH)_2$) tends to precipitate at the steel surface, and this product may undergo further reactions to form different forms of hydroxides and oxides depending on the availability of oxygen and water and the pH.

A schematic illustration of the process is shown in Fig. 2.1. Metal oxidation occurs at one site, called an anode, leaving free electrons in the metal. These electrons are then consumed at another site, called the cathode, by oxygen in the presence of water. The corrosion cell can be viewed as an electric circuit comprising four components: an anode, a cathode, an ionic conductor (pore water) and an electronic conductor (steel bar).

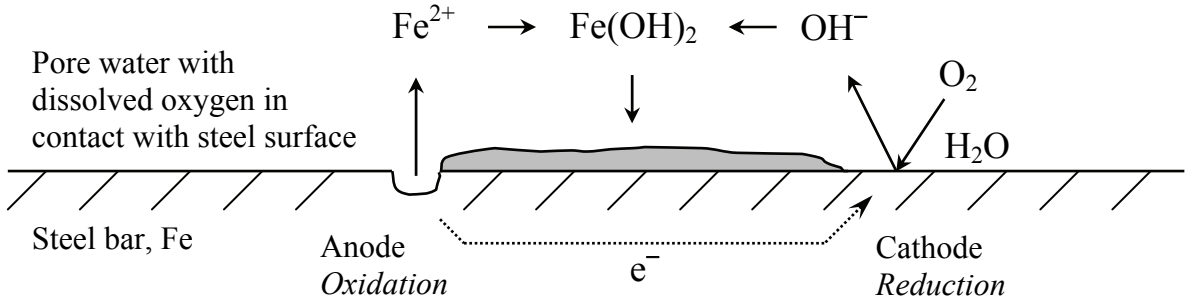

Figure 2.1 A schematic illustration of a steel corrosion cell in concrete.

Reaction kinetics

As electrochemical reactions imply transport of electric charges (ions and electrons), the rates of such reactions are normally given as electric current densities:

- Electric current = electric charges per unit of time (coulomb/s = ampere)
- Electric current density = electric current per unit surface area of steel (ampere/square meter)
- Corrosion current density = electric current density (microampere/square centimetre, $\mu A/cm^2$)

The corrosion current densities of steel in concrete may vary a lot – in the range of 10^{-2} to 10^2 $\mu A/cm^2$; very low current densities indicating passivity (Chapter 2.2) and higher current densities indicating active corrosion (Chapter 2.4).

Using Faraday's law of electrochemical equivalence, the corrosion rate in terms of amount of steel dissolving and forming hydroxide/oxide may be calculated from the electric current:

$$m = i \cdot t \cdot a / n \cdot F \tag{2.5}$$

where:

m = mass of iron per area dissolved at the anode (g/m^2)
i = electric current density (A/m^2)
t = time (s)
a = atomic mass of iron (55.8 g/mol)
n = number of electrons liberated in the anodic reaction (2 for $Fe \rightarrow Fe^{2+} + 2e^-$)
F = Faraday's constant (96487 As/mol)

Assuming the mass density of iron to be 7.87 kg/dm^3, the Faraday's law can be expressed as:

$$V_{corr} = 11.6 \cdot i_{corr} \tag{2.6}$$

where:

V_{corr} = corrosion rate (μm/year)
i_{corr} = corrosion current density ($\mu A/cm^2$)

In other words, a corrosion current density of 1 $\mu A/cm^2$ corresponds to 11.6 μm steel section loss per year.

Measurement of corrosion rate

There are various electrochemical techniques for measuring the rate of corrosion. Normally, the polarisation resistance, R_P (see below), is determined and the corrosion current density is calculated. In principle, the values from these measurements may then be used to calculate the metal section loss according to Eq. 2.6 assuming uniform corrosion over that particular time average and measured area.

There are several devices for corrosion rate measurements on the market. Some are designed for measuring corrosion of steel in concrete. It should be noticed, however, that different equipments may give somewhat different values for the corrosion rate at exactly the same measuring spot. This is partly due to different principles of measurement and the degree of steel confinement obtained by the instrument during measurement. Thus, the conversion of corrosion current densities to corrosion rates (Eq. 2.6) may need some sort of calibration and/or modification depending on type of device used for the measurement. Further, it has been assumed that the actual corrosion current density can be about five times that measured with a polarisation resistance device [Broomfield 2003].

The polarisation resistance technique

During the measurement a sensor (with a moist sponge) is placed on the concrete surface, and the corrosion potential is registered. Then, an electrical signal (voltage or current) is impressed to the steel reinforcement. The steel response to this signal is registered and used for calculation of the polarisation resistance (R_P). The R_P value is then used to calculate the corrosion current.

In contrast to corrosion potential measurements, which are normally carried out in a grid pattern on the concrete surface, measurement of the corrosion current has to be carried out directly above a selected part of the steel reinforcement with a known diameter and length. The main challenge during the development of this technique has been to limit the impressed electric signal to a defined length of the steel bar. This has been solved by introducing a guard-ring electrode in the sensor which hinders the impressed signal to be scattered across the steel bar in an uncontrolled way. In order to calculate the corrosion rate it is important to know the size of the steel bar responding to the electric impulse.

Prior to the measurement the steel bar is in an undisturbed condition characterised by a corrosion potential or rest potential. If the steel bar with known length and diameter is stimulated electrically (called polarisation) by a small impressed voltage (change of rest potential) or by a small impressed current, the steel bar responds immediately by producing a small current (if the potential was changed) or changing the rest potential (if current was impressed). The size of the electrical response (potential change or current production) is linked in a quantitative way to the ongoing corrosion activity at the time of measurement. Hence, the resistance to polarisation expresses the corrosion activity. Small polarisation resistance indicates high corrosion activity.

There are several electrochemical techniques for determining the polarisation resistance (R_P), of which the two most common for concrete purposes are:

- Linear Polarisation Resistance (LPR)
- Galvanostatic Pulse

The galvanostatic pulse technique, a novel technique being more and more common, is based on a polarisation resistance calculation obtained from a mathematical treatment of the change in potential the first milliseconds after impressing a very short and small current pulse to the steel bar (analysis of the potential / time curve).

The LPR-method, which has dominated this field for many years, uses another technique to determine R_P. This method is based on an impressed change of the rest potential of the steel. If the measurement is carried out very near the rest potential (corrosion potential) it is a linear relationship between impressed voltage and the current response. By using an electronic instrument (potentiostat) the voltage can be impressed in steps or scanned roughly 0.1 mV/s from approximately 10 mV to the positive or negative side of the corrosion potential through the zero point to 10 mV at the other side. In this linear potential/current range, Ohm's law can be used to calculate R_P, which is the relation between impressed potential (ΔE) and the current response (ΔI):

$$R_P = \Delta E / \Delta I \tag{2.7}$$

According to basic corrosion theory the corrosion current (I_{corr}) is inversely proportional to the polarisation resistance:

$$I_{corr} = B / R_P \tag{2.8}$$

where:

B = a constant (volt)
R_P = polarisation resistance (ohm)

Let A be the surface area of the steel bar that has received the impressed signal, then, the corrosion current density is given by:

$$i_{corr} = I_{corr} / A = \{B/R_P\}/A = \{B/(\Delta E/\Delta I)\}/A = \underline{(B/A)(\Delta I/\Delta E)} \tag{2.9}$$

It is important to notice that the measured values are instant values representing the corrosion activity at the time of measurement.

Even though modern instruments for measuring corrosion current are computerised and can be operated in a user-friendly way, electrochemical knowledge and experience are needed to carry out the measurements in a correct way and to interpret the results.

Similar measurements may also be carried out by permanently installed sensors in the concrete adjacent to the steel bar. Also in this case the problem of signal confinement must be solved. Sometimes this is done by cutting the steel bar at the measuring site, a solution giving a well defined steel area. The disadvantage is of course that this steel is not longer representative for the main steel reinforcement. For instance, any macrocell activities would be turned off.

2.2 Passivity

Fortunately, steel embedded in high pH concrete without chlorides does not suffer from any noticeable corrosion attack even if sufficient moisture and oxygen are available. This is due to the spontaneous formation of a thin protective oxide layer on the steel surface in the highly alkaline pore solution of the concrete. This formation is provided by the corrosion reaction described above.

The oxide layer is very thin and dense and probably consists of gamma ferric oxide (γ-Fe_2O_3) [Hausmann 1967] or a mixture of ferric oxide and magnetite (γ-Fe_2O_3/Fe_3O_4) [Andrade et al 1995]. This surface oxide layer, being a physical barrier separating the metal from the adjacent electrolyte, is often termed the oxide film or the passive film.

As long as the passive film remains intact the corrosion current density is very low, probably in the range of 0.01 $\mu A/cm^2$. Using Faraday's law (Eq. 2.6), this corresponds to a corrosion rate, or loss of steel bar section, of approximately 0.1 μm/year. Hence, the corrosion rate is depressed to an insignificant low level by the passive film. This low corrosion rate maintains the protective passive film due to a slight dissolution of the iron oxides that form the passive film.

It should be noticed that there has been a lot of discussions on different theories explaining the mechanisms and nature of protective layers on iron and steel in various alkaline

electrolytes [Amaral et al 1999]. Borgard et al [1990] even suggest that the normal concept of passive film formation does not hold for steel in concrete, and that it is more likely that the protection is provided by mineral scales, high in calcium, that are formed on the steel surface.

2.3 Thermodynamics of corrosion

The likelihood of electrochemical reactions to proceed in a given environment is determined by chemical thermodynamics, i.e. the Gibbs free energy of formation, ΔG, of the compounds involved. In electrochemistry one operates with the term *electrochemical potential* or *voltage* (volt), rather than free energy (Joule). Free energy and electrochemical potential are related:

$$E = -\Delta G/nF \tag{2.10}$$

where:

E = electrochemical potential ($J/As = J/C = Nm/C = kgm^2/Cs^2 \overset{def}{=} volt = V$)
ΔG = free energy of reaction (J/mol)
n = number of electrons transferred during the reaction (2 for $Fe \rightarrow Fe^{2+} + 2e^-$)
F = Faraday's constant (96487 As/mol)

In other words, *volt* (V) is energy per electric charge. If $E > 0$ the electrochemical reaction is a spontaneous process which can start and proceed driven by its 'own energy'. The higher the numerical (positive) voltage, the higher is the driving force for that particular reaction. The voltage attributed to a corrosion cell (see Fig. 2.1) is given by

$$E_{cell} = E_{cathode} - E_{anode} > 0 \tag{2.11}$$

Corrosion technologists relate to electrochemical potentials in two main ways:

(1) Measuring and evaluating corrosion potentials, E_{corr}, of the material (metal). The corrosion potential is defined as the electrode potential spontaneously acquired by the corroding material in a particular environment [Heusler 1989]. The corrosion potential of steel in concrete is measured by a reference electrode, either placed at the concrete surface during measurement, or permanently embedded in the concrete for long-term monitoring.

(2) Influencing the electrochemical potential of the material by applying electric signals to the material. This is done by using electrochemical instruments and electric power sources. Such procedures are used either to protect the material (e.g. cathodic protection) or measuring the corrosion rate of the material (e.g. LPR technique).

The latter case (2) utilizes the electrochemical potential to act as a driving force that affects the rate of electrode reactions:

High potentials (towards positive values):	The anodic reaction is stimulated $Fe \rightarrow Fe^{2+}$ accelerates The cathodic reaction rate decreases
Low potential (towards negative values):	The cathodic reaction is stimulated $O_2 \rightarrow OH^-$ accelerates The anodic reaction rate decreases

The electrochemical potential, E, varies with temperature and concentrations (activities) of the species involved in the reaction. The effects of these variations can be calculated by the Nernst equation (which is a modification of Eq. 2.10). For the steel corrosion reaction in concrete (Eq. 2.4) the Nernst equation would be:

$$E_{cell} = E^{o}cell - \frac{RT}{nF} \ln \frac{\left[Fe^{2+}\right]\left[OH^{-}\right]^2}{\sqrt{p_{O_2}}} \tag{2.12}$$

where:

E_{cell} = electrochemical voltage (potential difference) of the corrosion cell (V)
E^{o}_{cell} = electrochemical voltage of the corrosion cell in the standard state (i.e. temperature = 25 ^{o}C, concentrations (activities) = 1)
R = gas constant (8.314 $JK^{-1}mol^{-1}$)
T = temperature (as ^{o}K)
n = number of electrons transferred in the reaction (2 for $Fe \rightarrow Fe^{2+} + 2e^{-}$)
F = Faraday's constant (96487 As/mol)
$[Fe^{2+}]$ = concentration of Fe^{2+} in the electrolyte adjacent to the steel surface (mol/l)
$[OH^{-}]$ = concentration of OH^- in the electrolyte adjacent to the steel surface (mol/l)
p_{O2} = partial pressure of oxygen in the electrolyte adjacent to the steel surface (atm). For air in equilibrium with the electrolyte, p_{O2} = 0.2 atm

The Nernst equation has been used to construct *potential-pH* diagrams which indicate the conditions under which the metal is likely to corrode or not. These diagrams, based on equilibrium thermodynamics, are called Pourbaix diagrams [Pourbaix 1974], and they define three regions in the potential-pH space [Borgard 1990]:

(1) *Immunity region*
The metal is thermodynamically stable and is immune to corrosion.

(2) *Corrosion region*
Ions of the metal (Fe^{2+} and Fe^{3+} in the case of iron) are thermodynamically stable, and, under most conditions, corrosion will occur at a rate which cannot be predicted thermodynamically.

(3) *Passivity region*
Compounds of the metal are thermodynamically stable. These compounds, or passive films, may protect the substrate from further reactions with the environment.

The Pourbaix diagram for steel is shown in Fig. 2.2. Notice that this diagram is a thermodynamic diagram and therefore does not indicate the rate at which the most stable state will be achieved. We can see from Fig. 2.2 that the steel will be protected by a passive film at high pH, and that this protection can be lost at pH below 9 depending on the potential of the steel. The sloping, dashed lines (a) and (b) in Fig. 2.2 give the potentials of solutions in equilibrium with hydrogen and oxygen respectively.

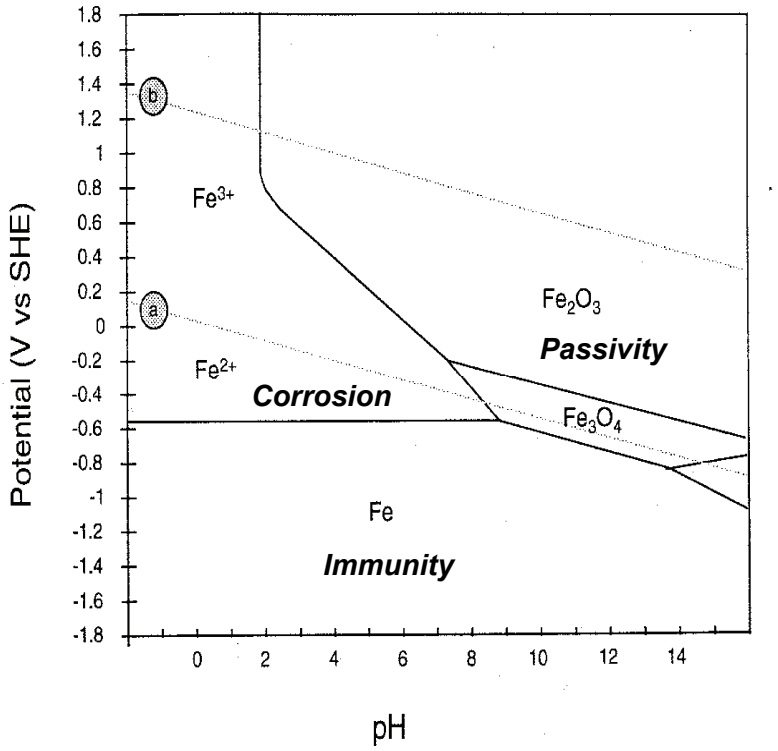

Figure 2.2 Simplified Pourbaix diagram for iron in water showing the most stable products at a given pH and potential [Pourbaix 1974].

2.4 Depassivation and active corrosion

The passive state is maintained as long as the concrete pore water in contact with the reinforcement is sufficiently alkaline and free from chloride ions. Provided the electrochemical potential of the steel is not kept at very low 'immune' values (see Fig. 2.2), the protective passive film is destroyed, a phenomenon called depassivation, if

- the pore water in contact with the steel drops to a pH level of about 9 (normally as a result of carbonation)

and/or

- the pore water in contact with the steel contains dissolved chloride ions above a certain threshold level.

Then, unless the steel is repassivated (either by increase in pH or removal of dissolved chloride ions) the corrosion rate normally increases by several orders of magnitude, and the structure suffers from active corrosion. Two main types of active corrosion are seen in concrete:

Localized corrosion (macrocell corrosion, pitting corrosion)

- Typically a few square centimetres (or even square millimetres) of corrosion, i.e. local anodic dissolution of iron, surrounded by large areas of passive steel bar acting as the cathode
- This is a typical characteristic of chloride induced corrosion. Chloride induced pitting corrosion is schematically illustrated in Fig. 2.3.
- Macroscopic separation of the anodic and cathodic reaction sites
- Pit formation with small concentrated anodes fed by large cathodes
- Macrocell corrosion rate depends on the electrical resistivity of the concrete, i.e. the ability of the concrete to transport electric charges (ions) between the anode and the cathode. High corrosion rates at large anode-cathode separations are possible only if the resistivity is sufficiently low.

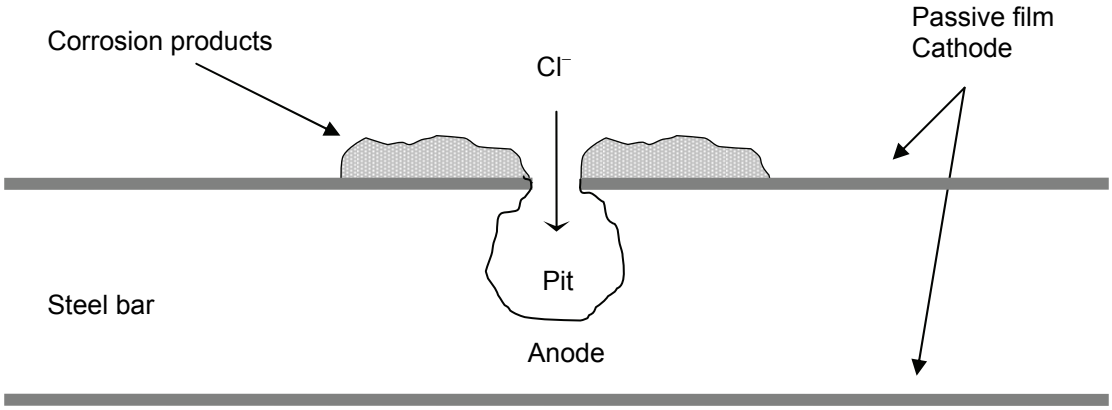

Figure 2.3 A schematic illustration of chloride induced pit formation on steel in concrete.

The moisture inside the pit may be very acidic due to the ability of ferrous ions (Fe^{2+}), in the presence of chloride, to split water molecules and form acid – hydrolysis of ferrous ions and hydrochloric acid formation:

$$Fe^{2+} + H_2O + Cl^- = FeOH^+ + HCl \quad (2.13)$$

Further, anodic dissolution of iron may now be fed by reduction of H^+ as the cathodic reaction, rather than reduction of oxygen:

$$2H^+ + 2e^- = H_2 \text{ (gas)} \quad (2.14)$$

General corrosion (microcell corrosion)

- Uniform corrosion attack over large areas
- No macroscopic separation of anode and cathode
- This is a typical characteristic of corrosion initiated by pH-drop (carbonation)
- In the presence of excessive amounts of chloride a large number of very closely situated pits may form and cause an almost uniform and even attack over the entire steel surface.

3 Factors affecting the corrosion rate

3.1 Environmental and material parameters

There are several factors which affect the corrosion rate of steel reinforcement in concrete. No comprehensive and satisfactory treatment of this complexity has been found in the literature. However, at least eight factors may influence the corrosion rate:

$$V_{corr} = \mathrm{f}\,(T, F_{O2}, RH, C_{Cl}, pH, \gamma, F_{galv}, F_{oxide}) \tag{3.1}$$

where:

T = temperature
F_{O2} = supply of oxygen to the pore water in contact with the cathodic area of the steel surface
RH = relative humidity in the concrete pores (or the degree of pore water saturation)
C_{Cl} = concentration of dissolved chloride ions in the pore water in contact with the anodic areas of the steel surface
pH = alkalinity, or the concentration of OH^--ions in the pore water in contact with the steel surface
γ = electrical resistivity of the concrete
F_{galv} = galvanic interactions between different parts of the steel reinforcement
F_{oxide} = effect of oxide (rust) layer formation on corrosion rate

Temperature, T

Temperature affects the corrosion rate directly, as for all chemical reactions. A general rule of thumb is that 10°C increase in temperature roughly doubles the chemical reaction rate. However, other non-chemical parameters involved in the total reaction (e.g. resistivity) may alter the temperature dependence. Anyhow, the rate of corrosion increases significantly with increasing temperature at normal ambient temperature range, but at high temperatures (probably around 40°C), the corrosion rate starts to decrease due to lack of oxygen (the solubility of oxygen decreases with increasing temperature).

Oxygen supply, F_{O2}

Being a reactant in the corrosion reaction, the corrosion rate is directly dependent on the supply of this reactant to the cathodic area of the steel. The rate of this supply is dependent on concrete porosity (P), the degree of moisture content in these pores (RH), the concrete cover thickness (d) and the temperature:

$$F_{O2} = \mathrm{f}(P, RH, d, T) \tag{3.2}$$

Information on the numbers, sizes and lengths of interconnecting pores supplying the steel with oxygen is given by P and d. High P and low d increase the rate of oxygen supply. However, a lot of investigations have showed that the moisture content has the highest impact on oxygen supply [Page 1982, Broomfield 2003]. For atmospherically exposed concrete structures the porous system is partly open, which allows transport of oxygen in the gaseous state. This transport is fast compared to the diffusive oxygen transport in water filled pores. In fully submerged structures the supply of oxygen is so low that the corrosion rate becomes very low, even in the presence of high C_{Cl}. A RH-value as high as 95 % does not restrict the oxygen supply significantly, while at 100% the 'starvation' of oxygen is significant. It should, however, be noticed that intense pitting can result even with a limited oxygen supply if the anode/cathode area ratio is high and the resistivity is low [Arup 1983] (see discussion on resistivity below).

Relative humidity, RH

The moisture content of the pore system affects the corrosion rate in three different ways:

- The corrosion reaction can only proceed in liquid water, and water is a reactant that is consumed in the reaction. This requires a minimum of moisture in the pores in contact with the steel. If the pores dry out, the electrochemical reaction stops.
- The corrosion rate depends on oxygen supply, which in turn depends on the moisture content of the concrete (see above).
- The corrosion rate depends on the electrical resistivity of the concrete. Resistivity depends on the moisture content of the concrete (see below).

The amount of water in the pores is a result of direct exposure to external water and variations in the local climate (moisture, temperature and wind).

Chloride concentration, C_{Cl}

As described above, depassivation occurs when the concentration of chloride ions dissolved in the pore water in contact with the steel reaches a threshold value. Reported threshold values scatter a lot, and it is not always clear which factors are operating or predominant regarding a specific threshold value for a given concrete structure or part of structure [Angst 2007].

The rate of the subsequent active corrosion is affected by the parameters described above. In addition, the active corrosion rate is increased by increasing amount of chloride present, i.e. the number of pits may increase, and almost uniform corrosion may be the result (see

discussion above), leading to an overall increase in the corrosion rate at a given steel surface area. Fig. 3.1 shows an example.

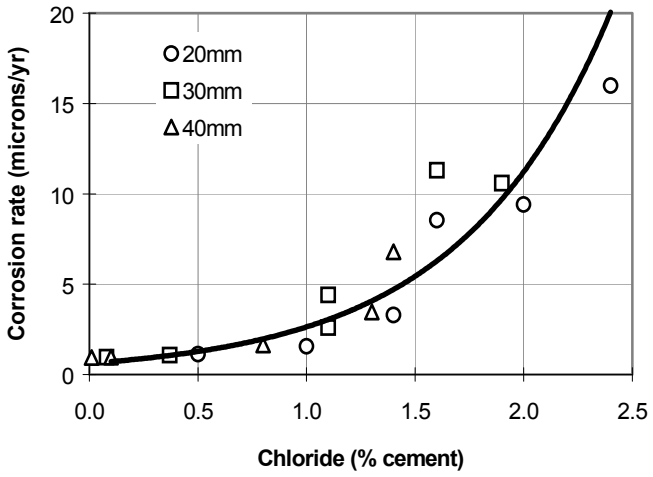

Figure 3.1 An example of the relationship between corrosion rate and total chloride content in the concrete at different cover thicknesses [Bamforth 1994].

Vassie [1984] reported data from UK bridges (see Fig. 3.2) and found that chloride contents below 0.2 % by weight of cement gave a low percentage of corroding steel bars (~20 %). As the chloride levels increased above 0.2 %, the proportion of corroding steel associated with each level of chloride increased in a way which is consistent with a normal distribution of threshold levels.

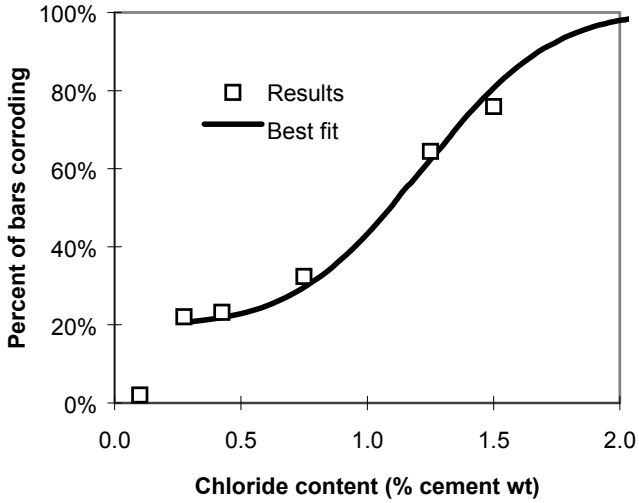

Figure 3.2 Corrosion activity as a function of chloride content [Vassie 1984]

The concentration of dissolved chloride is influenced by temperature, pH, moisture content and the capacity of the cement to bind chloride. Chloride ions can react with C_3A in cement to form calcium chloroaluminate, sometimes referred to as Friedel's salt [Neville 1995]:

$$3CaO \cdot Al_2O_3 \cdot CaCl_2 \cdot 10H_2O \tag{3.3}$$

Chemically bound chloride (C_{bound}) does not contribute to corrosion. The solubility of bound chloride increases with decreasing pH. This allows bound chloride to partly dissolve in carbonated concrete. The total amount of chloride (C_{total}) in the cement paste consists of both dissolved and bound forms:

$$C_{total} = C_{Cl} + C_{bound} \tag{3.4}$$

From this one may conclude that the concentration of chloride ions in the pore water in contact with the steel is a function of several factors:

$$C_{Cl} = f\,(T,\ C_{total}, C_3A\text{-content},\ pH,\ RH) \tag{3.5}$$

Alkalinity, pH

Besides affecting the passivity of the steel (see above), the pH of the concrete pore water may affect the corrosion rate in three ways:

- The corrosion cell potential or driving force (see Eq. 2.12) increases with decreasing pH
- A decrease in pH increases the dissolution of chemically bound chlorides, which may lead to an increase in the chloride induced corrosion rate (see above).
- An increase in the concentration ratio $[Cl^-]/[OH^-]$ may increase the corrosion rate [Hausmann 1967]. A lowering of pH will increase this ratio.

Although temperature affects alkalinity to some extent, the effect can be ignored when dealing with normal fluctuations in ambient temperature range.

Resistivity, γ

The electrical resistivity (ohm·m = Ωm) of the concrete affects the rate of electric current (or migration of ions) driven by the potential differences between the cathodic and anodic areas (see Eq. 2.11). This current is equal to the rate of corrosion. Hence, the corrosion current may be controlled by the resistivity. Low resistivity favours migration of ions. Low resistivity also favours the development of corrosion pits [Arup 1983], and the cathode/anode area ratio may become very large (because ions will easily migrate from cathodic areas at far distances from the anodic area – in the range of a meter).

The moisture content in the pores has a significant effect on the resistivity. The higher the moisture content and the higher ionic strength of the moisture, the lower is the resistivity. To some degree porosity also affects the resistivity:

$$\gamma = f\,(T,\ RH,\ ionic\ strength,\ P) \tag{3.6}$$

Research indicates that the single most important factor affecting the corrosion rate of depassivated reinforcement is the resistivity of the concrete. This is, in turn, influenced by the mix composition and the moisture content of the concrete. Fig. 3.3 illustrates the effect of temperature and relative humidity on rust formation in carbonated concrete.

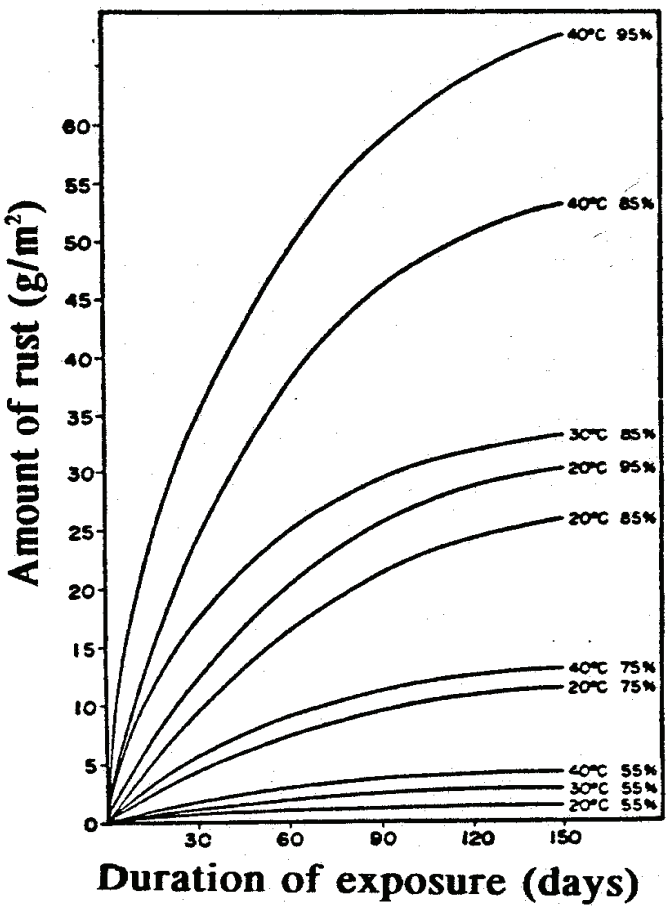

Figure 3.3 Effect of temperature and relative humidity on rust formation in carbonated concrete [Parrott 1987]

Galvanic interactions, F_{galv}

Although the term galvanic corrosion, in a strict sense, refers to corrosion at the contact point of two different metals or alloys with different potentials, researchers working on modelling of corrosion rates in concrete often use the term 'galvanic effects' or 'galvanic interactions' to describe the effects of macrocells on the corrosion rate [Gulikers 2006].

A galvanic macrocell is a corrosion cell where an active rebar (anode) is separated from a passive rebar (cathode). The passive rebar may accelerate the corrosion attack at the active rebar as a consequence of the potential difference between the two rebars. This macrocell action increases as the difference in the electrochemical potentials between the anodic and cathodic areas increases. Bertolini et al [2004] describes three examples of such macrocells in concrete:

- The most typical example would be a depassivated rebar (due to chloride penetration or carbonation) connected to a passive rebar. This type of macrocell action can give about 10 % increase in corrosion rate in high-resistivity concrete, while more than 90 % increase is reported for low-resistivity concrete.
- Epoxy-coated reinforcement may give rise to macrocell action if there are defects in the coating and the coated bars are electrically connected with uncoated passive steel bars in deeper parts of the structure.
- Patch repairs of chloride-contaminated concrete sometimes give rise to unwanted macrocells. After the repair, the formerly chloride-contaminated anodic zone becomes passive, and will no longer provide protection to the surrounding cathodic area. Due to small amounts of chloride in the formerly cathodic areas 'just outside' the repaired zone, corrosion can initiate in areas surrounding repaired zones (sometimes called 'incipient' anodes).

Rust layer formation, F_{oxide}

Steel in a passive state is covered by a very thin and dense layer of iron oxides (see Chapter 2.2). Unlike this passive film, rust layers formed on the steel surface during active corrosion are thick and porous and may consist of different types of iron oxides. Gulikers [2006] suggests that the continuous formation of rust and its aging influences the corrosion rate of the steel rebar.

For metals in general, the corrosion rate is normally highest at the beginning of an exposure. Later, it often becomes reduced due to the accumulation of more or less protective corrosion products on the metal surface [Wranglén 1985].

On the other hand, Novak et al [2001] found high corrosion rates on pre-rusted steel in concrete, and suggested that the rate of oxygen penetration through the concrete cover governs the corrosion rate. Indeed, it has been stated that the rust layer may favour corrosion both by providing a reducible material (iron oxides) for the cathodic reaction and by acting as a porous electrode for the reduction of oxygen [González et al 2007]. This is supported by the fact that iron oxides may act as efficient electro-catalysts for the reduction of oxygen in alkaline solutions [Vago and Calvo 1994].

3.2 Influence of cracks

Current predictive models assume that the concrete is uncracked. However, it is generally accepted that cracks, which are normally present in field concrete, promote more rapid penetration of aggressive agents (carbon dioxide, chloride) and may thereby adversely affect long-term integrity.

When dealing with corrosion in cracks, two different mechanisms are possible:

- Microcell corrosion; the anodic and cathodic processes take place only in the cracked zone. The anodes and cathodes are very small and can hardly be separated. The oxygen supply to the cathodes is through the crack.

- Macrocell corrosion; the reinforcement within the crack-zone acts mainly as an anode and the passive steel surface outside the crack acts as cathode. The oxygen transport to the cathode takes then place mainly through the uncracked concrete area.

Much higher corrosion rates are to be expected for the macrocell corrosion mechanism as much larger steel surface zones are involved in this cathodic process compared to the microcell corrosion mechanism. Several investigations on concrete elements exposed to chlorides clearly indicates that the reinforcement in the vicinity of cracks acts anodically whereas the reinforcement embedded in uncracked concrete show a cathodic behaviour, i.e. a macrocell corrosion , [Vennesland and Gjørv, 1981, Makita et al 1980, Okada and Miyagava 1980]. The same corrosion mechanism is expected to be decisive for carbonation induced corrosion as well.

The orientation of cracks with respect to the reinforcement plays an important role in determining their influence on corrosion. Where the crack is perpendicular to the reinforcement (transverse cracking), the corroded length of the intercepted bars is limited, whereas when cracks follow the line of a reinforcing bar (longitudinal cracking) they are likely to be much more damaging because the corroded length of the bar will be much greater.

Investigations have shown that the time to depassivation increases with decreasing crack width (transverse cracking). However, after depassivation the quality and depth of the concrete cover in the vicinity of cracks is much more decisive than a restriction of crack widths [Atimtay and Ferguson 1974, Raupach 1996c, Okade and Miyagawa 1980, Schiessl and Brauer 1996].

Further, self-healing has been shown to play a major role in the case of very fine static cracks exposed to wetting [Shiessl and Brauer 1996, Clear 1985]. However, in the case of dynamic cracks the rate of corrosion is larger than for static cracks [Schiessl and Brauer 1996, Hodgkiss et al 1984].

As crack frequency determines the number of potential corrosion sites it would be expected that the total reinforcing bar loss increases with increased frequency of intersecting cracks. Based on experimental investigations Arya and Ofori-Darko [1996] suggested that an effective measure against corrosion may be to limit the frequency of intersecting cracks by increasing the depth of cover to the reinforcement, rather than by controlling surface crack widths.

In Duracrete [1998] the following simple mathematical expression is proposed for the estimation of corrosion risk in cracked reinforced concrete members:

$$k = \frac{1}{c \cdot \rho} \tag{3.7}$$

where:

k = corrosion rate parameter
ρ = concrete resistivity (Ωm)
c = depth of cover (m)

The expression (Eq. 3.7) is based on common experience showing an inverse relation between corrosion damage and both resistivity and cover depth. However, the model has no practical value in its present form as it does not permit the comparison between corrosion behaviour in cracked and uncracked concrete.

4 Modelling of reinforcement corrosion

4.1 Corrosion rate

Numerous models have been proposed for predicting the onset and the rate of corrosion of steel reinforcement in concrete exposed to chlorides and carbonation. Maruya et al [2003] refer to three types of approaches used in modelling the corrosion rate in the propagation period:

- Models based on electrochemistry
- Models related to a diffusion-limited access of oxygen (see Eq. 3.2)
- Models in the form of empirical relations (e.g. based on electrical resistivity of the concrete)

Models based on electrochemistry

Complex corrosion models based on electrochemical principles and Butler-Volmer kinetics have been developed [Maruya 2003, Kranc and Sagüés 2001, Sagüés et al 1993, Kranc and Sagüés 1993]. These models are not yet sufficiently developed and they are impractical for practising engineers due to the high level of details required - e.g. knowledge of where pits will localize, future variations in relative humidity in the concrete, etc. Simpler models are required.

It is well known that the corrosion rate may vary with time. Accordingly, a penetration attack function, $P(t)$, representing the loss of rebar diameter at time t, has been developed [DuraCrete 2000]:

$$P(t) = \int_{t_i}^{t} V_{corr}(\tau) d\tau \tag{4.1}$$

where $V_{corr}(\tau)$ is the corrosion rate at the instant τ, and t_i the initiation period. This function gives the progress of corrosion with time as a function of the corrosion rate V_{corr} (mm penetration per year). This expression, however, can not be used as such by engineers to predict deterioration rates.

The time-independent expression for the corrosion rate, V_{corr}, described in Chapter 2 (Eq. 2.6) may be used to develop a more simple penetration attack. Assuming a uniform and constant corrosion rate during the propagation period, the progressive loss of rebar diameter (attack penetration) can then be expressed by the simple penetration attack function:

$$P(t) = V_{corr}\, t = 11.6\, i_{corr}\, t \qquad \text{[mm]} \tag{4.2}$$

Eventually, taking localized or non-uniform corrosion into account, this function has been modified by a so-called pitting factor, α [DuraCrete 2000]:

$$P(t) = V_{corr}\, t\alpha = 11.6\, i_{corr}\, t\alpha \qquad \text{[mm]} \tag{4.3}$$

However, the corrosion rate is usually not constant but evolves due to the corrosion process itself (progressive production of rust and extension of the corroded area) and due to climate variations. Therefore, a representative, or average, value of the corrosion rate, $V_{corr,a}$, first has to be determined. There are three possibilities of establishing $V_{corr,a}$ [DuraCrete 2000]:

1. To assume values in function only of the exposure classes (and not of the type of attack)
2. To estimate $V_{corr,a}$ from direct measurements of i_{corr} (in specimens for new structures or on-site for existing ones)
3. To use empirical expressions based on a variable governing the process, e.g. the electric resistivity of the concrete

The quantification of the first mode of determination of the corrosion rate, depending of the exposure class, can be given as [DuraCrete 2000]:

$$V_{corr} = V_{corr,\,a} \cdot w_t \tag{4.4}$$

$V_{corr,\,a}$ is the mean corrosion rate when corrosion is active and w_t is the wetness period, i.e. the fraction of the year that corrosion is active.

The second mode of determining the corrosion rate can be obtained, as described above, from direct measurements of i_{corr} and convert the measured result using Faraday's law. The factor 11.6 can be taken as deterministic. In order to incorporate differences obtained by different electrochemical measuring testing techniques, Eq. 2.6 is modified [DuraCrete 2000]:

$$V_{corr} = 11.6\, i_{corr}\, k_t \tag{4.5}$$

Here, i_{corr} corresponds to the value obtained by the measuring equipment, and k_t is a correction factor linked to that specific equipment or test method.

Note that different measuring equipment may give different values for the corrosion current density, even when measured at the very same spot. Liu and Weyers [1998] tested two commercial devices (3 LP and Gecor) – both are based on the Linear Polarization Resistance (LPR) technique – and found a significant difference in measured corrosion current densities. A difference factor of 15 was found, and it appears that the 3 LP overestimates the corrosion rate and the Gecor underestimates the corrosion rate.

Models related to a diffusion-limited access of oxygen

As described in Chapter 3.1, the access of O_2 at the steel surface in the cathodic zone of the rebars may be insufficient to fuel the corrosion reaction at high rate. The main factors affecting the supply of oxygen are the cover thickness of the concrete, the concrete porosity and the degree of water saturation in the concrete, the latter being the most crucial.

Kobayashi [1991] found that when moisture content of concrete (degree of pore saturation) is lowered from 80 % to 40 %, the value of O_2 diffusion coefficient becomes approximately 15 times higher.

Sudjono and Seki [2000] report that the coefficient of O_2 diffusion in very low or almost zero for water contents over 80 %. They found a nearly linear decrease in the coefficient with increasing water from 0 to 80 %.

Hence, the rate of corrosion may be dependent on O_2 diffusion. Under such conditions the highest corrosion current density possible, i_{corr}, equals the limiting current density of O_2 reduction, i_{lim}. The limiting current density may be calculated by combining Faraday's law (electrochemistry) and Fick's first law of diffusion (mass transport):

$$i/nF = -D_{O2}(dC^*_{O2}/dx) \tag{4.6}$$

where:

i = cathodic current density ($\mu A/cm^2$)
n = number of electrons transferred in the cathodic reaction (=4)
F = Faraday's constant (96487 As/mol)
D_{O2} = efficient diffusion coefficient of O_2 in concrete (m^2s^{-1})
C^*_{O2} = concentration of O_2 (mol/m^3)
x = distance (m)

Assuming a linear reduction of oxygen concentration from the surface of the concrete to the surface of the steel, and an oxygen concentration at the steel surface that is approximately zero due to the rapid reduction of oxygen, Eq. 4.6 may be rearranged and expressed as:

$$i_{lim} = 4FD_{O2}C_{O2}/d \quad (4.7)$$

where:

i_{lim} = limiting current density
C_{O2} = atmospheric oxygen concentration
d = concrete cover; oxygen diffusion path

Raupach [1996a, 1996b] investigated the influence of oxygen on the corrosion rate of steel in concrete using laboratory tests and calculations based on a model similar to Equation 4.7. He concluded that the diffusion of oxygen through the concrete cover is only a significant limiting factor for corrosion rate when the concrete is water saturated.

In a recent study, Huet et al [2007] reported oxygen diffusion behaviour in a CEM I paste with a water/cement ratio of w/c = 0.35 at varying moisture contents and cover thicknesses. They developed a more complex numerical model (compared to Eq. 4.7) to calculate the oxygen reduction current density, i_{O2}:

$$i_{O2} = C_{O2} / \{(1/k) + (d/D_{O2})\} \quad (4.8)$$

where k is the kinetic constant of oxygen reduction depending on several parameters like porosity and diffusion coefficient.

Based on Eq. 4.8, Huet et al [2007] constructed Fig. 4.1. From this study they concluded:

- For pore water saturation degrees (S_r) below ≈ 0.8 the calculated oxygen reduction limiting current is very high (≈ 200 μA/cm^2), and not consistent with experimental corrosion rate results. Thus, cathodic limitation of the corrosion process is not relevant. The rate limiting mechanism at $S_r < 0.8$ is the anodic reaction (anodic reaction control).
- In the intermediate range of S_r (≈ 0.8 – 0.9) both mechanisms (cathodic limitation control and anodic reaction control) must be taken into account.
- For water saturation degrees ≈ 0.9 the cathodic reaction is under diffusion control, but the oxygen diffusion rate is high enough to sustain reduction rates in the order of 10 μA/cm^2.
- In the water saturation range ≈ 0.9 – 1.0 the cathodic reaction is under diffusion control and depends therefore on the concrete cover thickness.
- The oxygen reduction rate under diffusion control decreases more than four orders of magnitude when S_r is increased from 0.9 to 1.0.

This investigation clearly shows that the degree of pore water saturation in the cement paste and its influence on diffusion properties are key parameters to assess corrosion rates. Thus, it is of great importance to couple electrochemical reactions on the reinforcement to transport of species that play a part in the electrochemical reactions, once active corrosion is initiated [Huet et al 2007].

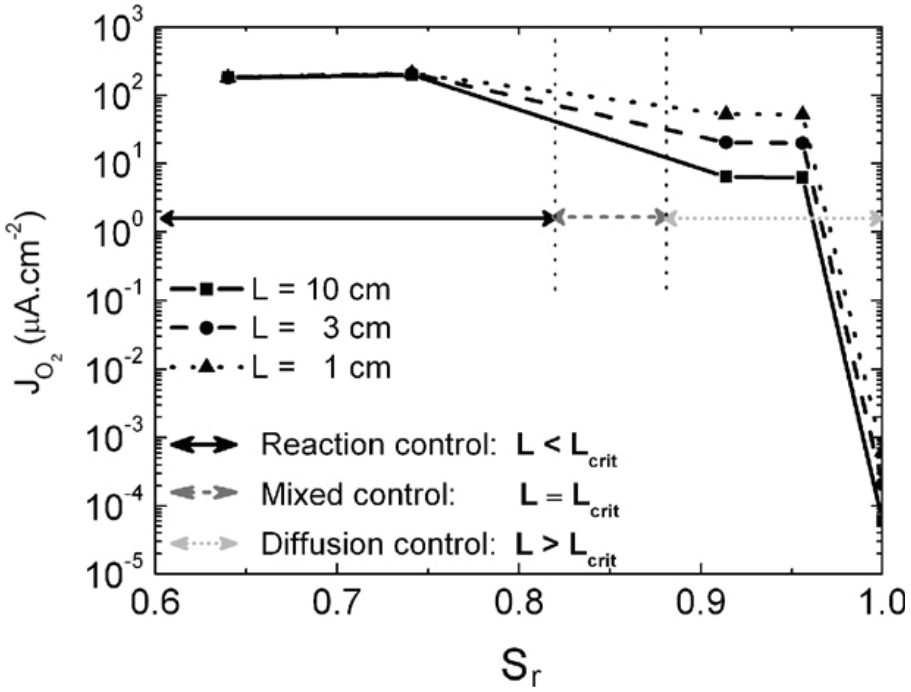

Figure 4.1 Evaluation of oxygen reduction rates (current densities) as a function of degree of pore water saturation (S_r) for three cover thicknesses, L (1, 3 and 10 cm) [Huet et al 2007].

Vennesland and Gjørv [2006] found that the rate of oxygen reduction at steel embedded in water saturated concrete is independent of the distance from the concrete surface to the steel (cover thickness).

Models in the form of empirical relations

Corrosion rates may also be predicted using empirical models. One basic approach to empirical modelling has been proposed in the DuraCrete project [DuraCrete 2000]:

$$V_{Corr} = \frac{m_o}{\gamma} \cdot \prod F_i \tag{4.9}$$

where:

m_o = factor given by the corrosion rate versus electrical resistivity
γ = electrical resistivity of the concrete
F_i = factor influencing the local corrosion rate

In Chapter 3.2 eight parameters (including electrical resistivity) were identified as factors that influence the corrosion rate. Some of these, probably the most influential factors, have been incorporated into Eq. 4.9 [DuraCrete 2000]:

$$V_{Corr} = \frac{m_o}{\gamma(t)} \cdot F_{Cl} \cdot F_{Galv} \cdot F_{O_2} \cdot F_{oxide} \tag{4.10}$$

The factors F_{Cl}, F_{galv}, F_{O2} and F_{oxide} are the chloride corrosion rate factor, the galvanic effect factor, the oxygen availability factor and the oxide (rust) factor respectively.

Eq. 4.10 does not reflect basic electrochemical expressions for the electrochemical reactions involved (e.g. Butler-Volmer kinetics). Accordingly, Eq. 4.10 does not really reflect the true nature of the corrosion process, and it is assumed that serious difficulties will arise by extending empirical expressions simply by adding a number of correction factors [Gulikers and Raupach 2006].

The electrical resistivity of the concrete is assumed to have a major effect on the corrosion rate. Vu and Stewart [2000] state that the electrical resistivity is the governing factor when the ambient relative humidity is low. At high relative humidity, however, the oxygen availability at the cathode is the controlling factor. This effect of moisture content on the corrosion rate can be summarized as:

Relative humidity	Resistivity	Oxygen diffusion	Corrosion rate controlling factor
Very high	*Low*	*Low*	*Oxygen diffusion*
Low	*High*	*High*	*Resistivity*

Taking into account the effects of resistivity and oxygen diffusion, and assuming a relative humidity of 75 % and temperature of 20^{O}C, Vu and Stewart [2000] developed an empirical model which gives the corrosion current density at the start of the propagation period (at time t_0) as a function of water cement ratio and cover thickness:

$$i_{corr}(t_0) = 37.8(1-w/c)^{-1.64}/d \qquad [\mu A/cm^2] \tag{4.11}$$

where w/c is the water cement ratio and d is the cover thickness (cm).

According to Vu and Stewart [2000] the formation of rust products at the steel surface will reduce the diffusion of iron ions away from the steel surface, and the area ratio between the anode and the cathode is reduced as a consequence of the corrosion process. Accordingly, it is assumed that the corrosion rate will reduce with time. Base on data reported by Liu and Weyers [1998] a model was developed by Vu and Stewart [2000] which expresses the relationship between time since the start of corrosion (propagation time, t) and the corrosion rate:

$$i_{corr}(t) = i_{corr}(t_0) \cdot 0.85t^{-0.29} \qquad [\mu A/cm^2] \tag{4.12}$$

Inserting Eq. 4.11 into Eq. 4.12 gives:

$$i_{corr}(t) = 32.1(1-w/c)^{-1.64}t^{-0.29}/d \tag{4.13}$$

Obviously, these models are strictly related to the specific experimental set-up used to develop the models, and should not be used generally to predict corrosion activity with time.

Another empirical approach was carried out by Liu and Weyers [1998]. They examined several factors affecting the corrosion process and developed an interaction model to characterize the corrosion rate, which can then be adjusted to an equivalent value according to the exposure conditions of the structure. Their model was based on a 5-year corrosion study obtained from a partial factorial experimental design that simulates reinforced concrete bridges. They used two commercial devices developed for corrosion rate measurements in concrete (3LP and Gecor) to measure the corrosion current densities. Measured values were calibrated against mean corrosion rates from weight loss measurements. The following influencing factors where included in the empirical model of Liu and Weyers [1998]:

- Temperature
- Ohmic resistance
- Chloride content
- Exposure time

Based on almost 3000 measurements from 7 series of mixed-in chloride contaminated specimens up to 5 years of outdoor exposure, the following non-linear regression model was found:

$$\ln 1.08\, i = 7.89 + 0.7771 \ln 1.69\, C_{Cl} - 3006/T - 0.000116\, R_C + 2.24\, t^{-0.215} \qquad (4.14)$$

where:

i = corrosion rate measured with the 3LP device ($\mu A/cm^2$)
C_{Cl} = chloride content (kg/m^3 concrete)
T = temperature at the depth of steel surface (Kelvin)
R_C = ohmic resistance of the concrete cover between the 3LP sensor and the steel rebar (Ω)
t = time since start of corrosion (years)

The empirical models described above should be used with care as they estimate corrosion rates for the very specific cases in which they were developed. The models should not be used uncritically for other cases.

4.2 Reinforcing bar deterioration

Rate of rebar section loss

Using Eq. 4.2 ($V_{corr} = 11.6\, i_{corr} \cdot t$), the percentage reduction of the rebar section can be calculated as a function of time for a given corrosion rate. Assuming a constant corrosion rate over time, the number of years to reach a certain deterioration level can be predicted by a very simple model. Fig. 4.2 gives an idealized illustration of cross section loss. Combining this idealized situation with Eq. 4.2 one finds that after time t the initial diameter ϕ of the corroding rebar has been reduced to ϕ':

$$\phi' = \phi - 2 \cdot V_{corr}\, t = 2 \cdot 11.6\, i_{corr}\, t \tag{4.15}$$

The factor 2 in Eq. 4.15 implies that the diameter is twice the radius. A mathematical rearrangement of Eq. 4.15 gives the percentage rebar section loss, L (%), of an initial rebar diameter, ϕ (mm), after time t (years) when the rebar corrodes at rate i_{corr} ($\mu A/cm^2$):

$$L\,(t,\phi) = 100\{1 - (4/\phi^2)(\phi/2 - 0.0116\, i_{corr}\, t)^2\} \tag{4.16}$$

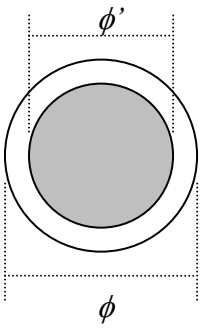

Figure 4.2 Reduction of rebar cross section as a result of corrosion.
ϕ = diameter of rebar before corrosion has started
ϕ' = diameter of corroding rebar at time t

Fig. 4.3 shows examples of calculated percentage loss of rebar sections (L) as a function of time. From these examples it is seen that if the corrosion rate is 10 $\mu A/cm^2$ a 30 % reduction in rebar cross section is reached in roughly 8 years for a rebar of 12 mm ϕ, while the same section loss for a rebar of 32 mm ϕ takes about 22 years. Andrade et al [1990] made similar calculations and deduced from this study that, in a corroding structure, a few rebars of large diameter seem safer than numerous thinner ones.

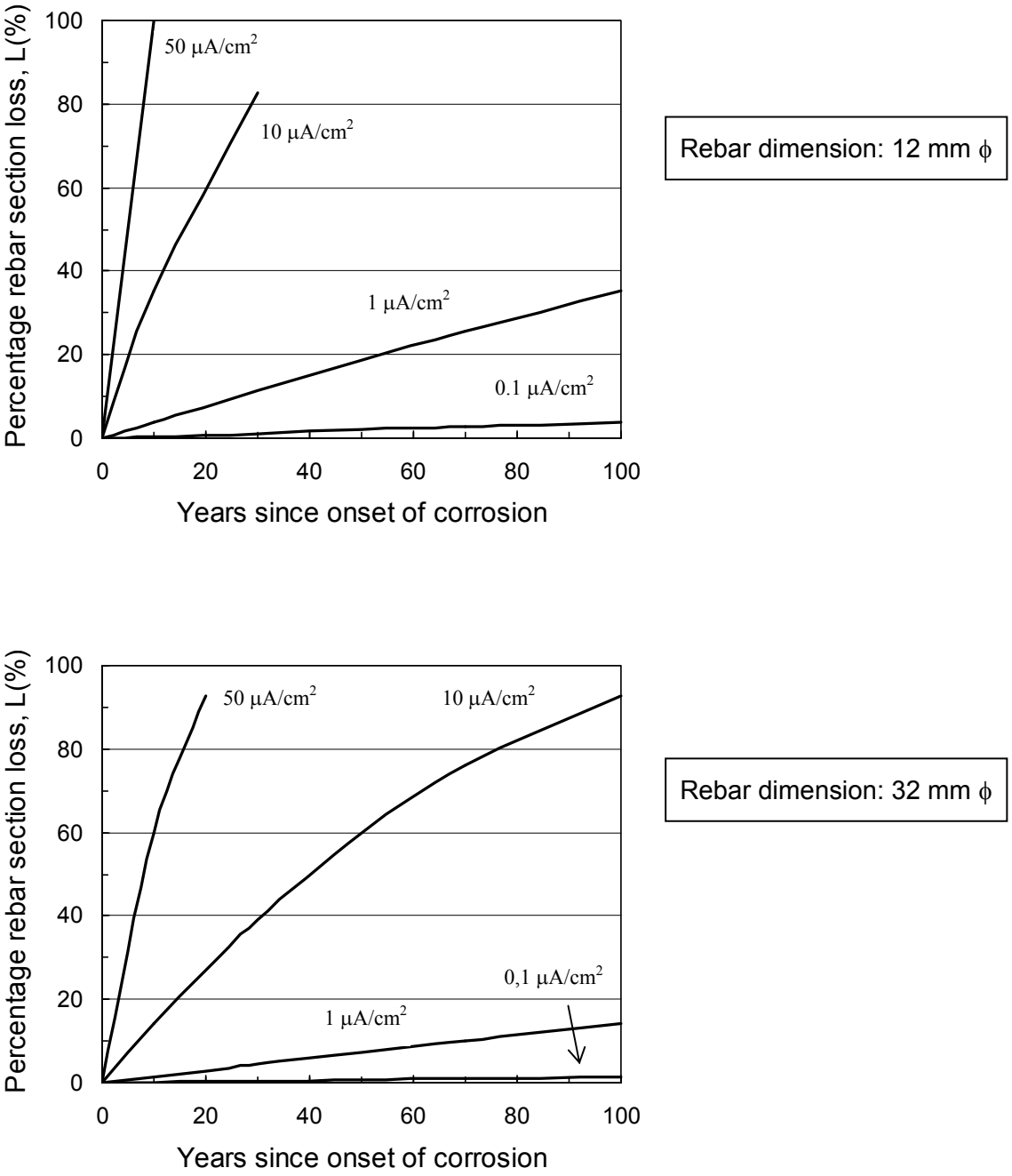

Figure 4.3 Percentage rebar section losses as a function of time, corrosion rate and rebar dimension (calculated by Eq. 4.15).

There exists some experimental evidence that the mechanical properties of the reinforcing steel may be affected by corrosion. The results obtained are, however, generally uncertain or contradictory.

Corrosion without volume expansion

It should be noticed that, under certain conditions, the corrosion products do not precipitate as solid oxides, but remain dissolved in the pore water. Dissolved corrosion products do not form expansive forces leading to cracking, but may diffuse into the pore system of the cement paste [Mehta 1991, Broomfield 2003]. High levels of pore water saturation and low levels of oxygen may lead to the formation of 'black' or 'green' rust – referring to the colour of the liquid seen on the rebar when first exposed to air after breakout. This type of corrosion may be found in deoxygenated conditions, particularly under membranes or when water is permanently ponded on the surface [Broomfield 2003]. This is a potentially dangerous form of corrosion as there is no indication of corrosion by cracking and spalling of the concrete. Accordingly, the reinforcing steel may be severely weakened before corrosion is detected.

Rust staining on a crack-free concrete surface may be indicative of this type of attack, but if water excludes oxygen it is unlikely that the iron in solution will get to the concrete surface where it will then precipitate out to form rust stains [Broomfield 2003].

4.3 Expansion and growth of corrosion product

Normally, the rust formed during corrosion causes volumetric expansions. Depending on the oxidation state of iron, the transformation of metallic iron to rust may be accompanied by a considerable increase in volume [Metha 1991]. Rust is a complex mixture of oxides, hydroxides and hydrated oxides of iron having a volume ranging from twice to about six times that of iron consumed to produce it [Broomfield 2003]. Any porosity in the rust will increase the volume further. Fig. 4.4 shows the relative volumes of different types of iron oxides assuming no porosity in the products. Type of oxide formed during corrosion is determined by pH, oxygen supply and moisture content in the concrete.

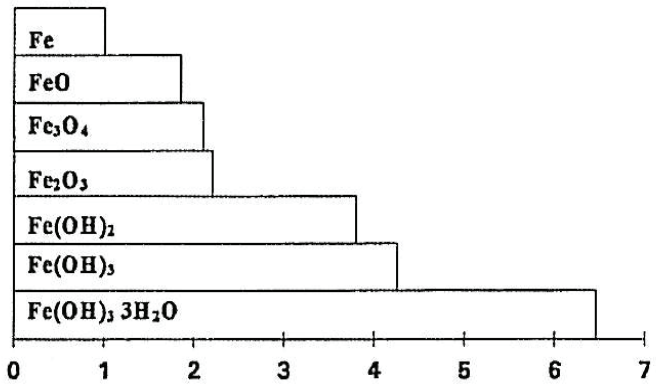

Figure 4.4 Relative volumes of metallic iron and its corrosion reaction products [Liu and Weyers 1998].

In their model, Duffó and Farina [2007] assumed that the mass of corrosion products increases linearly with time, an assumption that implies conservative time-to-cracking values. From Faraday's law and the chemical and physical data of steel bars, iron and its oxides, they

showed that the mass of corrosion products per unit length of the steel bar (W) produced at time t, is:

$$W = 2\pi \frac{i_{corr}}{n\,F} \cdot \frac{M_{rust}}{x} t \cdot \left(\frac{D_i}{2} - \frac{i_{corr} A_{Fe}}{n\,F\,\rho_{steel}} t \right) \tag{4.17}$$

where:

i_{corr} = corrosion current density
n = number of electrons transferred per ion
F = Faraday's constant
M_{rust} = molecular weight of the corrosion product
x = number of iron atoms in the chemical formula of the corrosion product
D_i = initial diameter of the steel bar
A_{Fe} = atomic weight of iron
ρ_{steel} = density of steel

However, according to Liu [1996] corrosion of steel in concrete is a dynamic process and the growth of corrosion products depends on the properties of the rust oxides and may follow different relationships with respect to time. For a metal that forms a protective oxide film, the rate of corrosion process will be retarded by diffusion of corrosion products through the film.

As the rust layer grows thicker, the rust production decreases because the diffusion rate is inversely proportional to the oxide layer thickness. Accordingly, Liu [1996] and Liu and Weyers [1998] described the rate of rust production as follows:

$$dW_{rust}/dt = k_p/W_{rust} \tag{4.18}$$

where:

W_{rust} = amount of rust products (mg/mm length of steel bar)
t = corrosion time (year)
k_p = rate of rust production

In their model, Liu and Weyers [1998] expressed the rate of rust production, k_p, as:

$$k_p = 0.098(1/\alpha)\pi D i_{corr} \tag{4.19}$$

where:

0.098 = numerical coefficient to fit experimental data
α = relation between atomic weight of iron (55.8) and the molecular weight of the rust product; e.g $\alpha = 0.523$ if the corrosion product is $Fe(OH)_3$
D = diameter of the steel bar (mm)
i_{corr} = annual mean corrosion rate (mA/ft^2)

5 Modelling of corrosion induced deterioration of concrete

5.1 Crack initiation and propagation

The concrete is a heterogeneous material where its porosity is dependent on the concrete quality. As corrosion products are generated they attempt to diffuse into the surrounding concrete. While some of the corrosion products may fill the voids or pores of concrete without generating pressure on the surrounding concrete, the remaining part may migrate away from the steel/concrete interface and, due to the expansion, generates bursting forces in the surrounding concrete. Cracks develop once the tensile strain capacity of the concrete is exceeded. Continued corrosion may then lead to further cracking and spalling of the concrete cover.

The corrosion induced cracking is illustrated in Fig. 5.1. Crack propagation is also influenced by additional factors including reinforcement detailing, external loading and environmental conditions.

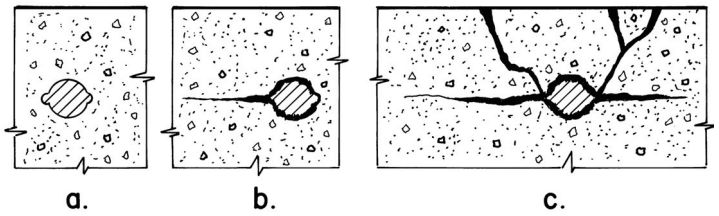

Figure 5.1 Corrosion-induced cracking of concrete [Daily 2007]
a. Steel rebar in the passive state
b. Delaminations within the concrete caused by rust growth
c. Spalling of concrete by expansive rust products

Most of the research work, which provides data regarding cracking of concrete cover and reinforcement corrosion, is limited to accelerated corrosion testing of reinforced concrete members carried out in the laboratory, e.g. Al-Sulaimani et al [1990], Cabrera and Ghodussi [1992], Andrade et al [1993], Clark and Saifulla [1994], Rodrigues et al [1994], Almumusallam et al [1996], Alonso et al [1998]. Table 5.1 compares section loss and corrosion penetration to the onset of cracking reported in various studies using impressed current techniques. The reported corrosion penetration that will generate enough expansive oxide growth to cause cracking is ranging from 6 to 130 μm. The results are, however, influenced by the test method including the level of impressed current, cover depth, reinforcing bar diameter, concrete properties, properties of rust products, etc.

Table 5.1 Corrosion penetration to cause cracking of concrete cover [***fib*** 2000]

Investigation	Bar dia. mm	Cover Ratio	Impressed Current mA/cm²	Section Loss %	Corrosion Penetration mm
Al-Sulaimani et al [1990]	20	3.75	2	2	0.10
	14	5.36	2	3	0.11
	10	7.50	2	5	0.13
Cabrera & Ghodussi [1992]	12	V. Large	3 Volts	1-2	0.03-0.06
Clark & Saifullah [1993]	8	0.5	0.5	0.4	0.008
	8	1.0	0.5	0.6	0.012
	8	2.0	0.5	1.3	0.026
Andrade et al [1993]	16	1.25-1.88	0.1	0.4-0.5	0.015-0.02
		1.25	0.01	0.45	0.018
Clark & Saifullah [1994]	8	1.0	2	0.3	0.006
	8	1.0	0.5	0.55	0.011
Rodriguez et al. [1994]	16	2.0 - 4.0	0.003-0.10	0.4 - 1.0	0.015 - 0.04
Almusallam et al [1996]	12	5.0	10	4.0	0.12

In the experimental investigation by Liu [1996], Liu and Weyers [1998] reinforced concrete members were cast with different amount of chloride mixed into concrete in order to simulate different corrosion rates. The water-cement ratios were between 0.43 and 0.45. The specimens were stored outside. The observed time to cover cracking ranged from few months to about 4 years depending of chloride content and concrete cover thickness. Table 5.2 shows measured corrosion rates, weight loss of reinforcement and observed time to cracking [Liu 1996].

Table 5.2 Measured corrosion rate, weight loss and observed time to cracking [Liu 1996]

No of specimens/ Admixed chlorides (kg/m^3 concrete)	Steel diameter (mm)	Cover depth (mm)	Measured corrosion rate ($\mu A/cm^2$)	Weight loss (mg/cm^2)	Observed t_{crack} (year)
3 / 5.7	16	48	2.41	39.3	1.84
3 / 5.7	16	70	1.79	60.1	3.54
4 / 7.2	16	27	3.75	29.8	0.72

In a review of models for predicting the attack penetration for onset of cracking of cover concrete under DuraCrete [1998] a relationship has been proposed that relates the amount of corrosion (attack penetration of the reinforcing bar to cause cracking) to the cover/bar diameter ratio and the splitting tensile strength:

$$x_{crack} = 83.8 + 7.4\ c/\phi - 22.6\ f_{c,sp} \quad (5.1)$$

where:

x_{crack} = attack penetration of steel (μm) to cause cracking
c/ϕ = cover/bar diameter ratio
$f_{c,sp}$ = characteristic value of the splitting tensile strength of the concrete [MPa]

In Eq. 5.1 the amount of corrosion required to cause cracking increases with cover depth and decreases with increasing reinforcement diameter, which is as reported in most experimental investigations. However, as the resistance of the concrete to cracking is strain-limited and not strength-limited the concrete tensile strength may not be the main parameter controlling the crack initiation. Moreover, in the relationship the unit is not correct, indicating that the parameter "tensile strength" should be replaced or combined with other mechanical concrete parameters.

Crack propagation due to corrosion, often presented as the crack opening (width) of the concrete, has been experimentally studied mostly using accelerated corrosion tests. An empirical expression giving the characteristic crack width is given by Rodriguez et al [1996] and adapted in Duracrete [1998]:

$$w = 0.05 + \beta \cdot [x - x_{crack}],\ [0 \le w \le 1.0mm] \quad (5.2)$$

where:

w = characteristic crack width [mm]
x = crack penetration (bar radius decrease) [μm]
x_{crack} = attack penetration leading to cracking initiation [μm] (see Eq. 5.1)
β = coefficient which depends on the position of the bar (β = 0.01 for top cast bars and 0.0125 for bottom cast bars)

The impact of simultaneous application of loading, which is thought to induce spalling [Rodriguez et al 1995a], is not included and nor is the effect of the presence of transverse reinforcement. Furthermore, whilst the expressions may be used for estimating the crack width value from the attack penetration, they are not applicable conversely, that is, to estimate the attack penetration value from the measurement of the crack width at the concrete surface.

In Al-Harthy et al [2007] a comparison between different empirical crack propagation models is shown; see Fig. 5.2.

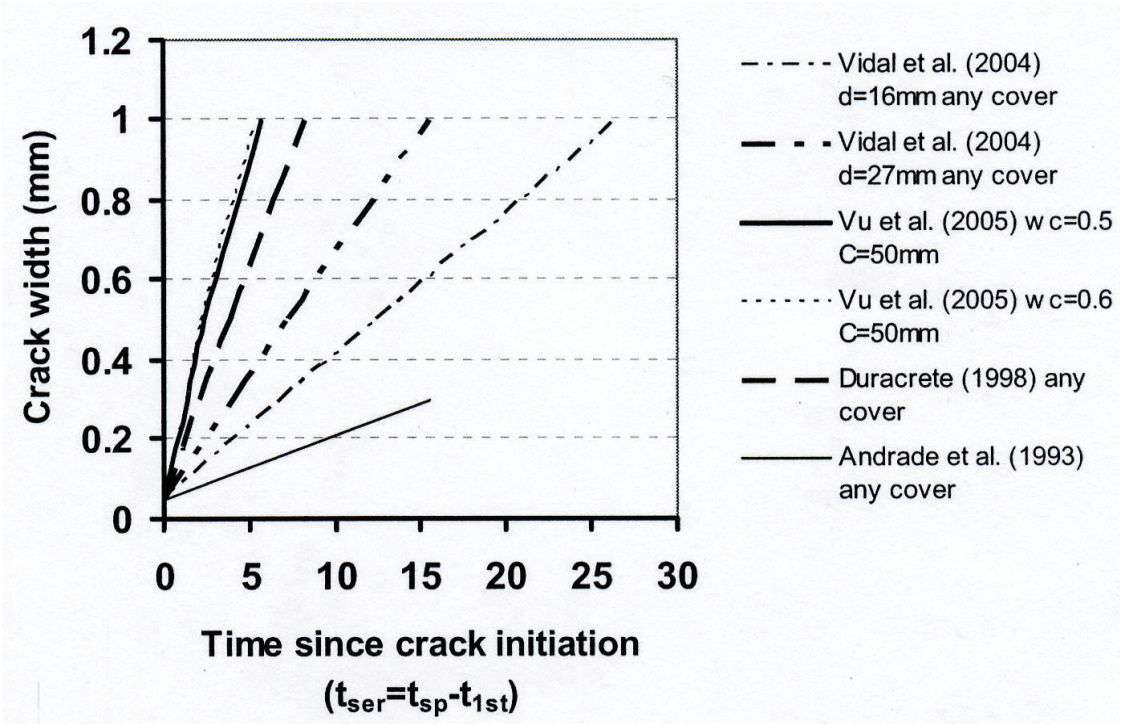

Figure 5.2 Comparison of predictions from crack propagation models [Al-Harthy et al 2007]. The corrosion density is 1 μA/cm^2. t_{ser} is the time (in years) since crack initiation and is calculated as $t_{ser} = t_{sp} - t_{1st}$, where t_{sp} is the crack propagation time measured/estimated from the start of the experiment or age of the structure, and t_{1st} is the time to crack initiation.

The large scatter in the model predictions of time since crack initiation is mainly due to differences in experimental procedures, assumptions and parameters used in the derivation of the models, along with the difference in member size and reinforcement layout, etc.

5.2 Time to corrosion cracking of concrete cover

Converting corrosion rate to cracking and delamination rate requires assumptions about expansive oxide growth and stresses required for cracking. Some examples are shown in Table 5.2. Of course, these simple time-to-cracking predictions are only indicative and should be used with care. In Table 5.3 it is assumed an on-going uniform rebar corrosion and an average rust expansion ratio of 3 (relative to metallic iron), i.e. the volume of rust occupies three times that of the original steel. Further, it is assumed that 50 μm section loss gives rise to cracking. This is in the range of tests results reported by Broomfield [2003]. A schematic illustration is shown in Fig. 5.3. Based on these simple assumptions and Eq. 2.6 (V_{corr}=11.6·i_{corr}), corrosion rates can be converted to annual rust growths and the time needed to cause cover cracking by the expansive oxides.

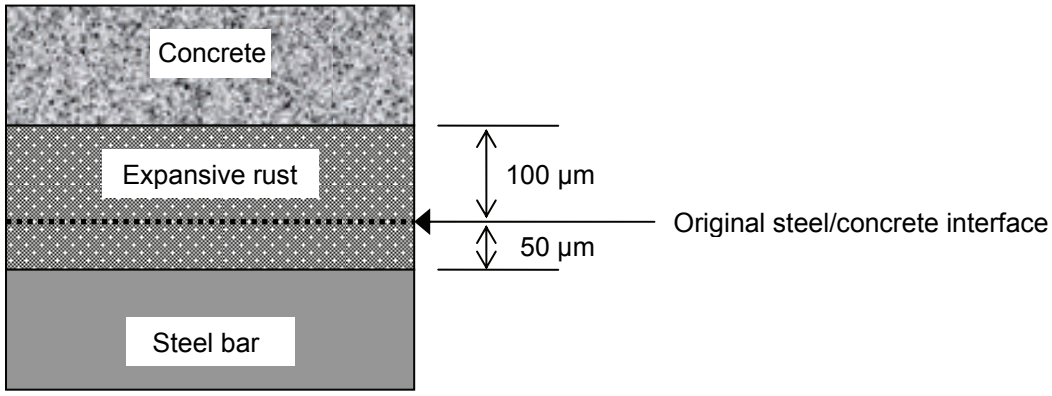

Figure 5.3 Schematic illustration of corroding rebar and expansive rust: 50 µm section loss of steel. Rust volume is three times that of the corroded steel (150 µm)

Table 5.3 Relation between annual rust growth and time from corrosion initiation to cracking of the concrete cover (Broomfield [2003])

Corrosion current density ($\mu A/cm^2$)	Rebar section loss (µm/year) *)	Rust growth **) (µm/year)	Time to cover cracking ***)
0.1	1.16	3.48	14 years
1.0	11.6	34.8	17 months
10	116	348	52 days

*) Calculated by Eq. 2.6 ($V_{corr} = 11.6 \cdot i_{corr}$)
**) Assuming three times expansion of iron oxides compared to metallic iron ($=3V_{corr}$)
***) Assuming that 50 µm rebar section loss is needed to cause cover cracking

According to Broomfield [2003], K. C. Clear made attempts, as early as 1976, to determine the time to cover cracking based on pure empirical data:

$$t_{crack} = \{(0.052\, d^{1.22}\, t^{0.21})/(C_s^{0.24}(\text{w/c}))\}^{0.83} \quad (5.3)$$

where:

t_{crack} = time to first cracking (years)
d = cover thickness (mm)
t = the age at which C_s was measured (years)
C_s = the surface (or near surface) chloride concentration (percent by weight of concrete)
w/c = water/cement ratio

The Clear model treats both the initiation period and time to cracking in one equation. This model has not been verified and the validity is questionable.

Based on field and laboratory data, an empirical equation was suggested by Morinaga [1988] to predict the time from corrosion initiation to corrosion cracking:

$$T_{cr} = \frac{0.602d\left(1+\frac{2c}{d}\right)^{0.85}}{i_{corr}} \tag{5.4}$$

where:

T_{cr} = time from corrosion initiation to cracking of cover concrete
c = concrete cover (mm)
d = diameter of the reinforcing bar (mm)
i_{corr} = corrosion rate in g/cm^2/day

According to Eq. 5.4 the time to cracking is a function of the corrosion rate, concrete cover depth and reinforcing diameter. However, the model does not include any effect of mechanical concrete properties.

In general, the difficulty with pure empirical relationships is to know the limitations and when they are valid.

One of the first analytical/mathematical models predicting the time from corrosion initiation to cover cracking including the effect of expansion of corroded steel and tensile properties was proposed by Bazant [1979]. In the model the concrete around a corroding reinforcing bar is considered as a thick-wall cylinder. The stresses in the cylinder wall, caused by formation of corrosion products having larger volume than the original steel, are calculated by means of isotropic linear elasticity theory. Further, cracking of concrete cover is assumed to occur when the stresses exceed the tensile strength of the concrete.

According to Bazant's model, time-to-cracking is a function of corrosion rate, cover depth, bar spacing, mechanical properties of concrete (tensile strength, modulus of elasticity, Poisson ratio and creep coefficient). A sensitivity study of Bazant's theoretical equation demonstrated that the corrosion rate is the most significant parameter in determining the time to cracking of the cover concrete [Liu and Weyers 1998]. The model has been validated experimentally and it was found to underestimate the time of first cracking [Liu and Weyers 1998].

The work by Bazant was extended by Liu and Weyers [1998]. Their model includes the same parameters used in Bazant's model, but it also includes the time required for corrosion products to fill an assumed porous zone at the steel/concrete interfaces before creating an internal pressure on the surrounding concrete. In their model the time from corrosion initiation to cover cracking, t_{crack}, is given as a function of the critical amount of rust product needed to induce cracking of the concrete cover, W_{crit}, and the corrosion rate, k_p:

$$t_{crack} = \frac{W_{crit}^2}{2k_p} \tag{5.5}$$

W_{crit} is modelled as:

$$W_{crit} = \rho_{rust}\left(\pi\left[\frac{Cf_t^{'}}{E_{ef}}\left(\frac{a^2+b^2}{b^2-a^2}+v_c\right)+d_0\right]D+\frac{W_{st}}{\rho_{st}}\right) \quad (5.6)$$

where:

ρ_{rust} = density of rust (corrosion) product
C = concrete cover depth
$f_t^{'}$ = tensile strength of concrete
E_{ef} = effective elastic modulus of the concrete; $E_{ef}=E_c/(1+\varphi_{creep})$
v_c = Poisson ratio
d_0 = thickness of the pore zone around the steel/concrete interface
D = original diameter of reinforcement
W_{st} = amount of steel loss
ρ_{st} = density of steel
a = $(D+2d_0)/2$
b = $C+(D+2d_0)/2$

In Liu-Weyers model [Liu and Weyers 1998] the rate of steel mass loss (or rate of rust production) caused by corrosion was assumed to decrease with time. However, the coefficients used were obtained by fitting experimental data.

Another critical parameter is the thickness of the pore band around the steel/concrete interface. They assumed a value of 12.5 μm in the validation of their model. However, according to Metha and Monteiro [1997], the interfacial zone may range from 10 to 50 μm in thickness. The sensitivity of this parameter is not studied. The predicted time-to-corrosion cracking was validated through observations made on time to cracking of reinforced concrete slabs with cast in chlorides exposed to an outdoor environment; see Table 5.2. So far, the model has not been verified against concrete structures under field exposure where chloride ions diffuse into the concrete.

The time to cover cracking as a function of concrete cover depth for different corrosion products and corrosion current densities is shown in Fig. 5.4 [Duffó and Farina 2007]. The predictions are based on Eq. 5.5 and Eq. 5.6 and assuming a linear relationship between corrosion current density and rust production.

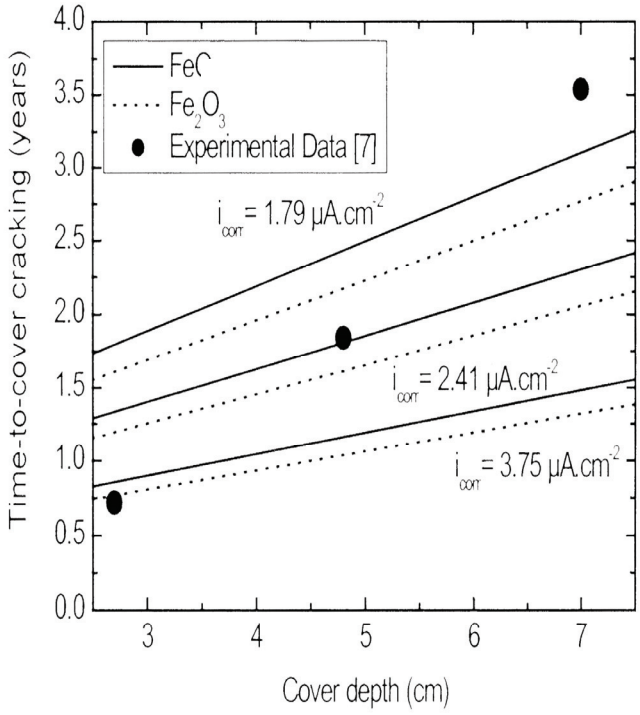

Figure 5.4 Predicted time-to-cover cracking as a function of the cover depth for different corrosion products and corrosion current densities [Duffó and Farina 2007]. The experimental data are from Liu and Weyers [1998].

A further refinement of the Liu-Weyers model was proposed by Bhargava et al [2006]. They modelled both the stiffness offered by the reinforcement and the corrosion product combined as well as the tension-softening (post-peak) behaviour of the cover concrete. The influence of the tensile softening behaviour of the concrete on the time to crack initiation was not reported.

It is believed that the tensile fracture energy of concrete is more important when modelling crack propagation and time to delaminating. This is confirmed by the analyses by Molina et al [1993], Hansen and Saouma [1999] where they modelled the cracking behaviour caused by corrosion by means of Finite Element Methods (FEM) including nonlinear fracture mechanics. In these models crack propagation is governed by energy considerations, and it was concluded that stable crack growth may occur prior to reaching the concrete surface. This means that additional expansion of corrosion products is necessary in addition to the expansion required to initiate cracks at the reinforcement concrete interface.

The mathematical models discussed above include several empirical coefficients which adjust the model prediction to experimental results from accelerated corrosion tests. The most sophisticated models need input parameters for the modelling of rust expansion (type of rust product and rate of rust production), rate of corrosion current, thickness of the pore zone band around the steel/concrete interface that can be filled by corrosion products without generating bursting forced in the concrete, etc. However, reliable values of such parameters are lacking.

6 Conclusions and further research

Corrosion of steel reinforcement in concrete is an electrochemical process strongly dependent on environmental factors and properties of the concrete. The overview of corrosion rate-determining factors clearly shows a complex relationship between many parameters. A number of factors have been identified to influence the corrosion rate alone. Hence, modelling corrosion of steel reinforcement in concrete based on mathematical models for the prediction of on-going corrosion kinetics in concrete would be a challenging task, taken into account the variety of influencing parameters and their fluctuations.

Modelling of the corrosion process in concrete needs a thorough knowledge of the evolution of corrosion with time. This would require sufficient long term outdoor testing of reinforced concrete members to account for the interaction of various environmental factors on the corrosion process. As the degradation is a long term effect, the experimental studies of corrosion are generally carried out under accelerated conditions. It is doubtful whether quantitative conclusions from theses studies can be reliably applied to real structures in the field.

Various studies show considerable variations in the extent of corrosion required to initiate cracking and the influence of cover thickness and steel bar diameter. A thorough understanding of governing mechanisms is needed to enable effective models to be developed.

Several formulae and models have been proposed for the calculation of the time to onset of cracking of the concrete cover caused by the reinforcement corrosion. Some analytical/mathematical models are deduced on the basis of mechanical principles and some empirical expressions are obtained according to the experimental data fitting.

So far the models for crack initiation and propagation have been restricted to the stresses generated by the expansion of corrosion products. Models comprising the total complexity of the problem, especially generated by load induced stresses, have not been found.

Most models include several empirical coefficients to adjust to experimental results from accelerated corrosion tests. The most sophisticated time-to-corrosion-cracking models (mathematical or based on Finite Element Methods) need input parameters for the modelling of rust expansion, rate of corrosion, amount of concrete pores that can be filled by corrosion products without generating bursting forced in the concrete, etc. However, reliable values of such parameters are lacking.

No reliable models for predicting the time to spalling or delamination of concrete are found. This phenomenon is governed by complex interactions between corrosion, loading conditions and reinforcement detailing, which are still not well understood.

Further research should focus on developing models based on electrochemical, chemical, physical and mechanical parameters only, without introducing numerical coefficients to fit empirical data. To do so, it is imperative to understand the relationships and mutual interactions between several parameters. Accordingly, basic research is needed, and several topics should be investigated more thoroughly before developing new models to predict corrosion induced concrete structure deterioration mechanisms:

- Effect of moisture, pH and concrete resistivity on corrosion rate
- Effect of moisture, oxygen, pH and chloride on type of rust formed during corrosion
- Effect of formation and growth of rust layers on the corrosion rate
- Effect of concrete porosity on rust growth and diffusion
- Effect of concrete quality on time to corrosion induced cracking
- Effect of inclusion of fibers on time to cover cracking and spalling
- See if there is possible to develop a technique to measure tensile strain in concrete caused by rust growth

Since the corrosion rate value is an important parameter in corrosion modelling, it is necessary to have reliable non-destructive corrosion rate measurement techniques for field use. More reliable devices for corrosion rate measurements in field are highly appreciated.

7 References

Al-Harthy, A.S, Mullard, J. and Stewart, M.G. (2007): Cracking in concrete due to corrosion of steel reinforcement", CONSEC, 07, Proc. ed. F. Toulemonde et al, Tours, Frence pp 383-390

Almumusallam, A., A. Al-Gahtani, A.S., Aziz A.R. and Rasheeduzzafar (1996): "Effect of reinforcement corrosion on bond strength", Construction and Building materials, Vol. 10, No.2, pp 123-129.

Alonzo, C. Andrade C., Rodriguez, J. and Diez, J. M. (1998) : "Factors Controlling Cracking of Concrete Affected by Reinforcement Corrosion", Materials and Structure*s,* V. 31, pp 435-441.

Al-Sulaimanti, G. J., Kaleemullah M. , Basunbul I.A. and Rasheeduzzafar (1990): Influence of corrosion and cracking on bond behaviour and strength of reinforced concrete memebers", Proceedings American Cocnrete Institute, Vol 87, No 2. Mar-Apr. pp 220-231.

Amaral, S. T. and Müller, I. L. (1999): "Passivation of pure iron in alkaline solution containing silicate and sulphate – Galvanostatic and Potentiostatic studies", Corrosion Science, Vol. 41, pp 747-758.

Andrade, C., Alonso, M. C. and Gonzalez, J. A. (1990): "An Initial Effort to Use the Corrosion Rate Measurements for Estimating Rebar Durability", in "Corrosion Rates of Steel in Concrete", ASTM STP 1065 (Berke, N. S., Chaker, V. and Whiting, D., Eds.), American Society for Testing and Materials, Philadelphia, USA, pp 29-37.

Andrade, C, Alonso C, and Molina F.J. (1993): "Cover Cracking as a Function of Rebar Corrosion. Part - 1 Experimental Test," Material and Structures*,* V.26, pp. 453-464.

Andrade, C., Merino, P., Nóvoa, X. R., Pérez, M. C., and Soler, L. (1995): "Passivation of Reinforcing Steel in Concrete", Materials Science Forum, Vols. 192-194, pp 891-898.

Angst, U. and Vennesland, Ø. (2008): "Critical chloride content. State of the art", SINTEF report SBF BK A07037, SINTEF Building and Infrastructure, Trondheim, Norway, 54 pp.

Arup, H. (1983): "The mechanisms of the protection of steel by concrete", in "Corrosion of Reinforcement in Concrete Construction" (Crane, A. P., Ed.), Ellis Horwood Limited, UK, Chapter 10, pp 151-157.

Arya, C. and Ofori-Darko, F.K. (1996): "Influence of Crack Frequency on Reinforcement Corrosion in Concrete." Cement and Concrete Research, Vol. 26, No. 3, S. pp. 345-353.

Atimtay, E. Ferguson, M. (1974): "Early Chloride Corrosion of Reinforced Concrete – A Test Report, In Materials Performance 13, No 12, pp 18-21.

Bamforth, P.B. (1994): "Specification and design of concrete for the protection of reinforcement in chloride contaminated environments. UK Corrosion and Eurocorr 94, Bournemouth, Vol. III, pp 249-258.

Bazant, Z.P: Physical Model for Steel Corrosion in Sea Structures – Theory", ASCE Journal of the Strucutural Division, Vo. 105, NO. ST6, pp 1137-1153.

Bertolini, L., Elsner, B., Pedeferri, P. and Polder, R. (2004): "Corrosion of Steel in Concrete. Prevention, Diagnosis, Repair", Wiley-VCH Verlag GmbH, Wienheim, Germany, Chapter 8, pp 125-134.

Bhargava, K, Ghosh, A. K., Mori, Y. and Ramanujam, S. (2006): "Model for cover cracking due to rebar corrosion in RC structures", Engineering Structures, Vol. 28, pp 1093-1109.

Borgard, B., Warren, C., Somayaji, S., and Heidersbach, R. (1990): "Mechanisms of Corrosion of Steel in Concrete", in "Corrosion Rates of Steel in Concrete", ASTM STP 1065 (Berke, N. S., Chaker, V. and Whiting, D., Eds.), American Society for Testing and Materials, Philadelphia, USA, pp 174-188.

Broomfield, J. P. (2003): "Corrosion of Steel in Concrete. Understanding, Investigation and Repair", Spon Press, London, UK, 240 pp.

Cabrera, J. G. and Ghodussi, P. (1992): "Effect of reinforcement corrosion on the strength of steel concrete bond", Proc. Int. Conf. on Bond in Concrete – from research to practice, Riga, Latvia, pp 10.11-10.14.

Clark, L. A. and Saifullah, M. (1993): "Effect of corrosion on reinforcement bond strength", Proc. Conf. on Structural Faults & Repair, Ed. Forde M. Engineering Techniques Press, Edinburgh, Vol. 3, pp. 113-119.

Clear, C. (1985): "The effects of autogenous healing upon the leakage of water through cracks in concrete", Technical Report 559, Published by the British Cement Association (formerly Cement and Concrete Association).

Daily, S. F. (2007): "Understanding Corrosion and Cathodic Protection of reinforced Concrete Structures", Corrpro Companies Inc., http://www.corrpro.com/pdf/CP48.pdf, 5 pp.

Duffó, G.S, and Farina, S.B. (2007): A model for the time-to-cover cracking od reinforced concrete due to rebar corrosion", International RILEM Workshop on Integral Service Life Modelling of Concrete Strucutres, Guimarães, Portugal, pp 277-284.

DuraCrete (1998): "Modelling of deterioration", BRITE EURAM, Probabilistic Performance based Durability Design of Concrete Structures, document BE95-1347/R4-5.

DuraCrete (2000): "Statistical Quantification of the Variables in the Limit State Functions", BRITE EURAM, Probabilistic Performance based Durability Design of Concrete Structures, Document BE95-1347/R9.

González, J. A., Miranda, J. M., Otero, E. and Feliu, S. (2007): "Effect of electrochemically reactive rust layers on the corrosion of steel in a $Ca(OH)_2$ solution", Corrosion Science, Vol. 49, pp 436-448.

Gulikers, J. and Raupach, M. (2006): "Preface. Modelling of reinforcement corrosion in concrete", Materials and Corrosion, Vol. 57, No. 8, pp 603-604.

Hansen, E.J. and Saouma, V.E. (1999): "Numerical simulations of reinforced concrete deterioration: Part II – steel corrosion and concrete cracking", ACI Mater J, 96 (3), pp 331-338.

Hausmann, D. A. (1967): "Steel Corrosion in Concrete. How Does It Occur?", Journal of Materials Protection, Nov, pp19-23.

Heusler, K. E., Landolt, D. and Trasatti, S (1989): "Electrochemical Corrosion Nomenclature", Pure & Appl. Chem., Vol. 61, No 1, pp 19-22.

Hodgkiess, T., Arthur, P.D., and Earl, J.C. (1984): "Corrosion fatigue of reinforced concrete in seawater", Materials Performance. Vol. 23, July, pp. 27-31.

Huet, B., L'hostis, V. L., Santarini, G., Feron, G. and Idrissi, H. (2007): "Steel corrosion in concrete: Deterministic modelling of cathodic reaction as a function of water saturation degree", Corrosion Science, Vol. 49, pp 1918-1932.

***fib* (2000):** "Bond of reinforcement in concrete", State-of-art report, Bulletin 10.

***fib* (2006):** "Model Code for Service Life Design", Model Code, Bulletin 34.

Kobayashi, K. and Shuttoh, K. (1991): "Oxygen diffusivity of various cementitious materials", Cement and Concrete Research, Vol. 21, pp 273-284.
Kranc, S.C. and Sagües, A.A. (1993): "Calculation of extended counter electrode polarization effects on the electrochemical Impedance response of steel in concrete" ASTM STP 1188, J.R. Scully, D. Silverman and M.W. Kendig Editors, pp. 365-383.

Kranc, S. C. and Sagüés, A. A. (2001): "Detailed modelling of corrosion macrocells on steel reinforcement in concrete", Corrosion Science, Vol. 43, pp 1355-1372.

Liu, T. and Weyers, R. W. (1998): "Modelling the dynamic corrosion process in chloride contaminated concrete structures", Cement and Concrete Research, Vol. 28, pp 365-379.

Lui, T (1996): "Modeling the Time-to-Corrosion Cracking of Concrete Cover Concrete in Chloride Contaminated Reinfroced Concrete Structures", PhD thesis, Virginia Polytechnical Institute and State University, Blacksburg, Va.

Makita, M., Mory, Y. and Katawaki, K. (1989): "Marine Corrosion Behaviour of Reinforced Concrete Exposed at Tokyo Bay", ACI, SP-65, In Performance of Concrete in Marine Environment, Detroit, Michigan, pp 271-290.

Maruya, T., Hsu, K., Takeda, H. And Tangtermsirikul, S. (2003): "Numerical Modelling of Steel Corrosion in Concrete Structures due to Chloride Ion, Oxygen and Water Movement", Journal of Advanced Concrete Technology, Vol. 1, No. 2, pp 147-160.

Mehta, P. K. (1991): "Concrete in the Marine Environment", Chapter 5, Taylor & Francis, UK, pp 72-102.

Metha, P.K. and Monteiro, P. (1997): "Concrete. Microstructure, Properties and Materials, 3rd Edn. (McGraw-Hill, New York).

Molina, F.J. Alonso C, and Andrade C. (1993): "Cover cracking as a function of rebar corrosion: Part 2 numerical model", Mater Struct, Vol. 26, pp 532-548.

Morinaga, S. (1988): "Prediction of service lives of reinforced concrete building based on rate of corrosion of reinforcing steel", Report No 23, Shimizu Corp, Japan.

Neville, A. (1995): "Chloride attack of reinforced concrete: an overview", Materials and Structures, Vol. 28, pp 63-70.

Novak, P., Mala, R. and Joska, L. (2001): "Influence of pre-rusting on steel corrosion in concrete", Cement and Concrete Research, Vol. 31, pp 589-593.

Okada, K., Miyagawa, T (1980); "Chloride Corrosion of Reinforcing Steel in Cracked Concrete", ACI, SP-65, In Performance of Concrete in Marine Environment, Detroit, Michigan, pp 237-254.

Page, C. L. and Treadaway, K. W. J. (1982): "Aspects of the electrochemistry of steel in concrete", Nature, Vol. 297, pp 109-115.

Parrott, L.J. (1987): "A review of carbonation in reinforced concrete", Carried out by the Cement and Concrete Association (now BCA) under a BRE contract.

Pourbaix, M. (1974): "Atlas of Electrochemical Equilibria in Aqueous Solutions", National Association of Corrosion Engineers, Houston, Texas, USA, pp 307-321.

Raupach, M. (1996a): "Investigations on the influence of oxygen on corrosion of steel in concrete – Part 1", Materials and Structures, Vol. 29, pp 174-184.

Raupach, M. (1996b): "Investigations on the influence of oxygen on corrosion of steel in concrete – Part 2", Materials and Structures, Vol. 29, pp 226-232.

Raupach, M. (1996c): "Corrosion of Steel in the Area of Cracks in Concrete-Laboratory Test and Calculations Using a Transmission-Line-Model." Cambridge: The Royal Society of Chemistry. Corrosion of Reinforcement in Concrete Construction, 4th International Symposium, Cambridge, UK, 1-4 July 1996 (Page, C.L.; Bamforth P.B.; Figg J.W.(Ed)), pp. 13-23.

Rodríguez, J., Ortega, L. M. and García, A. M. (1994): "Assessment of structural elements with corroded reinforcement", in "Corrosion and Corrosion Protection of Steel in Concrete" (Swamy, R. N., Ed.), Sheffield Academic press, UK, pp 171-185.

Rodríguez, J. Ortega L.M. Casal, J. and Díez, J.M. (1996) " Corrosion of reinforcement and service life of concrete structures*,"* International Conference on Durability of Building Materials and Components, Stockholm.

Sagües, A.A. Kranc, S.C. and Washington, B.G. (1993) "Computer modelling of corrosion and corrosion protection of steel in concrete," Concrete 2000, R.K. Dhir and M.R. Jones Editors, Dundee, Published by E&FN Spon, pp 1275-1284.

Schieβl, P. Brauer, N. (1996): "Influence of Autogenous Healing of Cracks on Corrosion of Reinforcment", In the International Conference on the Durability of Building Materials and Composites, Stockholm, Sweden.

Sudjono, A. S. and Seki, H. (2000): "Experimental and Analytical Studies on Oxygen Transport in Various Cementitious materials", in "Durability of Concrete. Proc. Fifth Int. Conf.", Vol II, (Malhotra, V. M., Ed.), USA, ACI International SP 192-44, pp 721-738.

Tutti, K. (1982): "Corrosion of steel in concrete", Swedish Cement and Concrete Institute, Stockholm, Sweden, CBI-report Fo4, 429 pp.

Vago, E. R. and Calco, E. J. (1995): "Oxygen electro-reduction on iron oxide electrodes: III. Heterogeneous catalytic H_2O_2 decomposition", Journal of Electroanalytical Chemistry, Vol. 388, pp 161-165.

Vassie, P.R (1984): "Reinforcement corrosion and the durability of concrete bridges", Proc. Instn. Civ. Engrs, Part 1, 76, pp 713-723.

Vennesland, Ø, Gjørv, O.E. (1981): "Effects of Cracks in Submerged Concrete Sea-Structures on Steel Corrosion", Material Performance, pp 49-51.

Vennesland, Ø, Gjørv, O.E. (2006): "Oxygen Reduction at Steel in Submerged Concrete - Galvanic Corrosion in Sea Water", presented at 2nd International Conference on Concrete Repair, St. Malo, France, June 27-29.

Visal, T., Castel, A, and Francois, R. (2004): " Analyzing Crack Width to Predict Corrosion in Reinforced Concrete", Cem and Concr Res, Vol. 34, pp 165-174.

Vu, K. A. T. and Stewart, M. G. (2000): "Structural reliability of concrete bridges including improved chloride-induced corrosion models", Structural Safety, Vol. 22, pp 313-333.

Vu, K. A. T., Stewart, M. G. and Mullard, J. (2005): "Corrosion-Induced Cracking: Experimental Data and Predictive Models", ACI Struicutral J. 102(5), pp 719-726.

Wranglén, G. (1985): "An Introduction to Corrosion and Protection of Metals", Chapman and Hall, London, UK, Chapter 16, pp 220-249.

SINTEF Building and Infrastructure is the third largest building research institute in Europe. Our objective is to promote environmentally friendly, cost-effective products and solutions within the built environment. SINTEF Building and Infrastructure is Norway's leading provider of research-based knowledge to the construction sector. Through our activity in research and development, we have established a unique platform for disseminating knowledge throughout a large part of the construction industry.

COIN – Concrete Innovation Center is a Center for Research based Innovation (CRI) initiated by the Research Council of Norway. The vision of COIN is creation of more attractive concrete buildings and constructions. The primary goal is to fulfill this vision by bringing the development a major leap forward by long-term research in close alliances with the industry regarding advanced materials, efficient construction techniques and new design concepts combined with more environmentally friendly material production.